U. of Iowa 65-10

Adiabatic Motion of Auroral Particles in a Model of the Electric and Magnetic Fields Surrounding the Earth*

by

Harold E. Taylor** and Edward W. Hones, Jr.+

April 1965

Department of Physics and Astronomy
University of Iowa
Iowa City, Iowa

*This work was supported in part by the National Aeronautics and Space Administration under grant NsG-233-62.

**Graduate Trainee of the National Aeronautics and Space Administration

+On leave of absence from the Institute for Defense Analyses, Washington, D. C.

ABSTRACT

The motion of charged particles in the electric and magnetic fields constituting the earth's magnetosphere is calculated using the assumption that the first and second adiabatic invariants are conserved. The model of the magnetic field includes the effects of the solar wind pressure on the sunward side of the magnetosphere and of the newly discovered current sheet in the magnetospheric tail. The electric field is deduced in the ionosphere from the SD current system which accompanies magnetic bays. The magnetic field lines are then assumed to be equipotentials so that the electric field can be projected throughout the magnetosphere. The motion of low energy plasma is discussed qualitatively while the motion of solar wind particles which become trapped on the surface of the magnetosphere is calculated in quantitative detail. It is found that solar wind electrons (kinetic energy at the magnetospheric surface < 1 keV) will be accelerated to energies in the range of 1 to 40 keV and will be confined to a narrow latitudinal zone where extensive precipitation into the atmosphere will occur during local nighttime. Protons of similar energy will be confined to a region south of the electron region and will precipitate during local afternoon and evening.

The conclusion is reached that auroral events are produced largely by electrostatic acceleration of solar wind particles and occur on lines of force which close in the tail of the magnetosphere within 50 R_E of the earth.

I. INTRODUCTION

A satisfactory understanding of geophysical phenomena such as auroras, magnetic storms, and trapped radiation belts will probably come about only through quantitative calculations of the motions of charged particles in the electric and magnetic fields which constitute the magnetosphere. Such calculations involve the use of a model of the magnetosphere and they can be expected to reproduce actual particle motions only to the extent that the model represents the actual fields. The fields are, today, only imperfectly known. Nevertheless we believe that calculations using a model based on the known features should provide reasonably accurate representations of gross features of actual particle motions, such as general flow paths and precipitation patterns.

The magnetometers on Explorers 10, 12, 14, and 18 (Imp I) [Heppner et al., 1963; Cahill and Amazeen, 1963; Cahill, 1964; Ness et al., 1964; Ness, 1965] have provided a good though incomplete description of the magnetic field. These measurements have revealed that the magnetic field has a well defined boundary on the sunward side of the earth's dawn-dusk meridian plane and is drawn out into a tail of undetermined length on the antisolar side. Ness et al. [1964]

have shown that the field undergoes a sharp reversal of direction near the center of the tail indicating a current sheet of considerable extent. The approximate intensity and direction of the field are known in the interior of the magnetosphere to distances of ~ 30 R_E (earth radii) from the earth. No direct measurements of the electric field have been made, but reasonable estimates of it in the ionosphere may be deduced from current systems which are inferred from magnetic disturbances observed on the ground. Both the magnitude and the direction of the field are sensitive to assumptions made about the conductivity of the ionosphere, the height of the currents, and the contribution of earth currents to the magnetic disturbances. Once a field is obtained in the ionosphere it may be projected throughout the magnetosphere by assuming that the conductivity perpendicular to the magnetic field lines is negligible compared to the conductivity parallel to them so that the field lines may be considered to be equipotentials.

In order to calculate the motions of particles we have constructed a model of the magnetosphere which exhibits the gross features described above. The electric field is the sum of that derived from the high-latitude SD current system and that due to charge separation caused by the rotation of the ionosphere with the earth. The calculation of particle motions

in the model of the field was done under the assumption that the first two adiabatic invariants and the total energy (kinetic plus potential) of the particle are conserved. We have also limited ourselves to lines of force which reach the earth at a magnetic latitude greater than 60°. Lower latitude lines of force are nearly dipolar in character and particle motions on these lines should be well represented by the use of a dipole field. Such studies have been carried out by Maeda [1964] and Hones [1965].

The magnetic field model used is a modification of that used in earlier calculations of particle drifts by Hones [1963]. A large image dipole limits the extent of the earth's magnetic field toward the sun and oppositely directed uniform fields, added above and below the magnetic equatorial plane, extend the magnetosphere's tail in a manner comparable with that observed by Ness [1964]. The University of Iowa's IBM 7040 computer was used to calculate magnetic field lines in this model as well as the needed values of the integral invariant.

Simple mapping of the electric field derived from SD current system and corotation effects into the equatorial plane of the model and into a cross section of its tail has provided certain insights into the patterns of circulation of

plasma in the earth's magnetosphere. These are discussed qualitatively. In a more quantitative vein, flow patterns of solar-wind protons and electrons, assumed trapped at the surface of the magnetosphere, have been determined and precipitation patterns of these particles on the earth traced out. Comparisons of the latter with particle measurements by satellites and rockets and with auroral observations lead us to conclude that the auroral particles--both electrons and protons--are solar-wind particles streaming through the magnetosphere, accelerated and precipitated by the action of electrostatic fields.

These calculations predict many of the observed features of auroras. Probably the most significant is the prediction of a zone of relatively narrow latitudinal extent on the night side of the earth in which 1 to 40 keV electrons will precipitate. Protons must precipitate to the south of this region where electrons are found thus providing an explanation for the separation of electron and hydrogen auroras observed in the evening [Rees, Belon, and Romick, 1961]. Another striking prediction is the sharp cutoff of low energy proton precipitation at the noon meridian. Such a cutoff has been observed by the Lockheed experimenters [Meyerott, 1964].

In addition to providing predictions which agree with observations these quantitative calculations cast doubt upon certain features of earlier qualitative explanations of geomagnetic phenomena. For instance, we believe that auroral events occur on magnetic lines of force which close in the tail of the magnetosphere within 50 R_E of the earth, not on lines of force which extend into the interplanetary medium. Also turbulence and random processes do not appear to be of primary importance in producing auroral particles.

In general the results provide strong justification for the use of adiabatic theory in studying particle behavior even in the more distant regions of the magnetosphere.

II. THE MAGNETIC FIELD

The model used for the magnetic field employs an image dipole to produce the effects of surface currents which limit the spatial extent of the field lines which emanate from the earth [Hones, 1963]. In addition, the field of an infinite uniform current sheet of finite thickness is added in the tail of the magnetosphere. The noon-midnight meridional cross section of the model is shown in Figure 1. The dipoles are oriented parallel to each other and are assumed to be perpendicular to the ecliptic plane. The current sheet was centered about the ecliptic plane and has a thickness of .5 R_E. The edge effects of the current sheet are neglected so that the magnetic field of the current sheet is just a uniform field parallel to the earth-sun line, directed toward the sun north of the ecliptic plane and away from the sun south of the ecliptic plane.

The magnetic moment of the image dipole and the distance between the two dipoles were adjusted to obtain the appropriate radial distance to the front boundary at the subsolar point.

An image dipole 28 times as strong as the earth's, placed 40 R_E away, caused the boundary of the magnetosphere to be at a radial distance of 10.8 R_E at the subsolar point.

The magnetic field strength at the subsolar point is 60 γ (1 $\gamma = 10^{-5}$ gauss). The field of the current sheet was taken to be 30 γ in the present calculation. (Subsequent calculations with weaker current sheet fields show no significant changes either in the integral invariants or in the configuration of the field lines.)

The intersection of the boundary of this model with the dawn-dusk meridian plane is nearly circular with a radius of about 17 R_E. The tail of the model magnetosphere is roughly cylindrical in shape although its thickness perpendicular to the equatorial plane does decrease slightly at larger radial distances. (At 40 R_E this thickness is approximately 30 R_E.) The half width in the equatorial plane remains ~ 17 R_E.

Ness's measurement with IMP-1 [Ness et al., 1964] shows that, near the ecliptic plane, the width of the magnetosphere increases as one moves away from the sun and appears to approach a maximum value of ~ 40 R_E at X = -20 R_E. (The coordinate system used throughout this paper is one in which the X-axis points toward the sun, the Z-axis is anti-parallel to the dipole moment of the earth, and the Y-axis is chosen to form a right-handed system. This corresponds to a solar ecliptic system since we have assumed the dipole axis to be normal to the ecliptic plane.) In the dawn-dusk meridian plane the width

appears to be ~ 26 R_E. The measured field intensity was 30 to 60 γ near the subsolar point.

For the calculations described in this report, it is important, not only to use a model whose dimensions and field intensities match those of the real magnetosphere, but also whose lines of force trace out the same paths as do those in the real magnetosphere. Unfortunately, there exists little evidence on which to base an estimate of the path followed through the magnetosphere by a line of force emanating from a chosen point on the earth. This is especially true of the high-latitude lines of force. Figure 2 is a view of the equatorial plane of our model showing the equatorial crossing points of lines of force from various longitudes. The draping back of the high latitude lines is evident. We have arbitrarily chosen to define as "closed lines" only those which cross the equator at distances less than 50 R_E. For example, in the midnight meridian plane, the line from 12.4 degrees co-latitude is the highest latitude "closed" line.

Our definition of "closed" lines results in there being at the polar cap of the earth a roughly circular region extending from ~ 9° co-latitude at noon to ~ 13° co-latitude at midnight from which emerge "open" lines, i.e., lines which extend beyond 50 R_E. This region is indicated in Figure 3,

which is a view of the north polar cap of the earth. (All subsequent polar diagrams in this report are also views from above the north pole.) In the tail the "closed" lines occupy a roughly wedge-shaped region centered on the equatorial plane. It extends the full width of the tail and has a thickness of ~10 R_E at X = -10 R_E, tapers to ~ 4 R_E at -25 R_E, and ends in a sharp edge at -50 R_E. Actually the choice of the distance to which a line must extend in order that it be considered open is not critical. A choice of greater distances (say 100 R_E or 150 R_E) does not significantly extend the latitude range of the closed lines at the surface of the earth since, in this model, a current sheet of infinite extent is assumed.

Some information about where lines of force go in the real magnetosphere can be obtained from the high latitude termination of energetic trapped particles if one assumes that these particles cannot be durably trapped on lines of force which penetrate the current sheet. Such lines, at least beyond ~ 10 R_E where the field of the current sheet is greater than the field of the earth's magnetic moment, will have a sharp radius of curvature (of the order of the thickness of the current sheet). Figure 3 indicates the region on the earth

from which emanate those lines of force which penetrate the current sheet at $X < -10\ R_E$. The low-latitude boundary of this region corresponds quite well with the high latitude boundary of trapping of > 40 keV electrons, reported by Frank, Van Allen, and Craven [1964], though some differences are seen, especially near the noon meridian. Frank et al. show the termination of trapping at noon to be at ~ 13° while the model would predict about 9°. Since the prediction depends on the position of the neutral point line, this appears to indicate that the neutral point in the real magnetosphere should be at about 12°. Calculations are now being carried out on a model which incorporates this modification. The present model, however, appears to be quite satisfactory in most respects. If one keeps in mind the fact that the real magnetosphere probably has a neutral point line at ~ 12° instead of ~ 9° as found in this model, some of the deviations between experiment and the calculations to be discussed are reduced.

III. THE ELECTRIC FIELD

Large-scale electric fields are generated in the magnetosphere by (a) ionospheric motions produced by gravitational action of the sun and moon, (tides), and by the sun's heating of the atmosphere; (b) the earth's rotation, carrying with it at least the lower levels of the ionosphere; and (c) interaction of the solar wind with the outer magnetosphere. Though the electric fields have not been measured directly, considerable knowledge about them has been gained from studies of geomagnetic field variations associated with the currents they produce in (and above) the ionosphere. The geomagnetic field undergoes two kinds of daily variation, with periods of a solar day and a lunar day. These are denoted by S and L. The L variation, due to gravitational effect of the moon, is very small and will not be discussed further. When the S variation is derived from magnetically quiet days (usually the five international quiet days of each month) it is denoted by Sq. When it is derived from disturbed days (usually the five international disturbed days) it is denoted by SD. (The Sq variations arise from the gravitational and heating action of the sun and their theory is quite well understood. The additional variation occurring on disturbed days is thought to be due to the solar

wind's action and is not understood theoretically. It is from the latter variation, however, that the electric field we use in these calculations is derived.) The disturbance daily variation, denoted by SD, is defined as the difference Sd-Sq. At high geomagnetic latitudes the variation, SD, is much greater than at low latitudes and S derived from the international quiet day records of high latitude stations generally contains an appreciable SD part. Chapman and Bartels [1951, p. 290] conclude that "the distribution and development of the disturbance field (SD) in polar regions, as well as in lower latitudes, remain fairly constant and independent of the intensity of the disturbance". (They add, however, that the high latitude region (above ~ 60° latitude) in which the strong SD currents flow appears to broaden and move towards lower latitudes during periods of intense disturbance.) Thus, to a first approximation, the pattern of currents causing the disturbance field may be regarded as having a constant shape but varying intensity and orientation. Silsbee and Vestine [1942], from a study of hundreds of magnetic bays observed at many stations during the Polar Year, 1932-33, constructed the disturbance field current system which is shown in Figure 4. The magnetic bays were not associated with storms but were

required, for selection in the study, to have a maximum horizontal intensity at least as great as the average disturbance daily variation (SD_i) for international disturbed days at each station. The current system of Silsbee and Vestine thus represents moderately disturbed (though not storm-time) conditions.

A model electric field, $\vec{E}$, was derived from the current system of Figure 4 by solving the equation,

$$\vec{J} = \overleftrightarrow{\sigma} \cdot \vec{E} . \qquad (1)$$

Here $\vec{J}$ is the height-integrated current flowing in the ionosphere and $\overleftrightarrow{\sigma}$ is the height-integrated conductivity tensor; values for the latter were taken from the work of Fejer [1953]. The electric field, appropriately integrated, provided the potential distribution which is shown plotted over the north polar cap in Figure 5. The orientation of this potential distribution with respect to the earth-sun line is one of its more notable features because the direction of the equipotential lines over the polar cap (within ~ 15 degrees of the pole) has been cited, in the past, as observational support for theories of magnetospheric convection which have been developed by Axford and Hines [1961] and by Levy et al. [1963]. [See also Axford (1964); Axford et al. (1965).] These theories suggest a streaming of plasma

forward (i.e., sunward) through the tail of the magnetosphere as a major feature of the convective motion there (induced, in the case of Axford and Hines, by viscous interaction at the magnetosphere boundary and, in the case of Levy et al., by breaking and re-connecting of the earth's polar field lines). They cite, as observational support, the alignment of the polar cap ionospheric currents toward the sun (equivalent to convection of plasma by an $\bar{E} \times \bar{B}$ drift away from the sun, driven by an electric field in the dawn to dusk direction across the polar cap). Polar cap current systems were reported to have approximately this orientation by Chapman and Bartels [1951] and by Chapman [1951]. However, the system of Vestine and Silsbee is directed about 65° to the west of the sun. A system directed 60° to 90° to the west of the sun was derived from studies of 346 weak, moderate, and great storms by Sugiura and Chapman [1960]. More recently Fairfield [1963, 1964] made a statistical study of the orientation and intensity of the very high latitude current system in quiet and disturbed times. He concludes that in quiet times it is directed most often ~ 65° west of the sun while it tends to point ~ 30° west of the sun during disturbed times. The time variations, both in intensity and direction, are large.

Observational evidence, thus, seems to suggest that if the very high latitude disturbance daily variation, SD, is attributable to ionospheric currents, these are, on the average, directed not toward the sun, but more nearly ~ 60 degrees from the sun. It is notable, also, that the equipotential system which one derives from the current system, when not only the Hall conductivity but also the direct conductivity is taken into account, is rotated even further (about 15°) westward. This may be seen by comparing Figures 4 and 5; thus, it appears that convection of plasma over the polar cap proceeds more nearly in the direction dawn to dusk than in the direction noon to midnight.

In addition to the electric field deduced from the observed currents, one must include the electric field caused by the charge separation induced by the rotation of the ionosphere with the earth. This electric field causes no currents in the reference frame rotating with the earth, but in inertial space it will exert a force on particles and thus must be taken into account. This field is the usual polarization field produced when a conductor moves in a magnetic field:

$$\vec{E} = -\frac{\vec{v}}{c} \times \vec{B} . \qquad (2)$$

The potential of this electric field for a dipole whose magnetic moment is parallel to the axis of rotation is

$$V_{COROT} = -\frac{1}{c}\,\Omega\,\mu_E\,\frac{\sin^2\theta}{R} \qquad (3)$$

where Ω is the angular velocity of rotation;
μ_E is the dipole moment;
θ is the co-latitude; and
R is the radial distance.

In the case of the earth's ionosphere this becomes

$$V_{COROT} \approx -92 \sin^2\theta \text{ (kilovolts)}. \qquad (4)$$

The effects due to the non co-alignment of the magnetic moment and the rotation axis can be calculated and are discussed later. In the calculations done in this study they were neglected. When this potential is added to the potential deduced from the SD currents the potential system in Figure 6 results. Notice that the addition of the co-rotation potential system does not alter the potential system drastically; that is, the SD electric field is considerably larger than the co-rotation field at latitudes above ~ 60°.

To find the spatial dependence of the potentials, and therefore the electric field, we make use of the assumption that

the magnetic field lines are equipotentials. This is done by assigning the value of the potential which a field line has in the ionosphere to every point in space which lies on that field line. Thus one obtains the potentials of all points in the magnetosphere. This process leads to the potential system shown in Figures 7 and 8. Figure 7 shows the intersection of the equipotential surfaces with the geomagnetic equatorial plane (which coincides with the ecliptic plane in our model). Figure 8 shows the intersection of the equipotential surfaces with the plane perpendicular to the earth-sun line 40 R_E from the earth in the anti-solar direction ($X = -40\ R_E$). The latter figure shows that the electric fields are directed radially outward from the axis of the tail. The radial aspect of the electric fields exists everywhere in the tail (i.e., $X \lesssim -10\ R_E$).

It is interesting to consider the motion of very low energy plasma in such a field. (By very low energy plasma we mean particles whose magnetic drifts are negligible compared to the $\bar{E} \times \bar{B}$ drift.) Viewed toward the earth from far back in the tail, the plasma will drift around the axis of the tail in a counterclockwise sense north of the current sheet and in a clockwise sense south of the current sheet. In the equatorial

plane the plasma will flow toward the earth on the evening side of the tail and away from the earth on the morning side of the tail. The plasma flow near the earth resembles that of a fluid entering the magnetosphere on the dusk side, flowing around behind the earth (presumably forced to do so by the earth's rotation), and leaving the magnetosphere on the dawn side. This flow is somewhat different from that proposed by Axford and Hines [1961] (compare with their Figure 5). The difference results largely from the orientation of the electric potentials we have used. We find, for example, the center of rotation in the tail is near the axis rather than on the morning side of the tail. This rotation center corresponds to the maximum in the potential at 15° co-latitude at ~ 0200 L.T. (see Figures 5 and 6). Another important difference is that our model does not show the backward (i.e., anti-solar) flow on the evening side of the tail which their model portrays. Nor is there indication of a strong forward flow through the center of the tail. In short, this model does not display the major features which would be caused either by viscous interaction with the solar wind at the boundary or by the breaking and re-connecting of field lines. Rather, the convection pattern has <u>qualitative</u> features which one would expect of

a system driven by the earth's rotation alone. Since the electric field is deduced from currents in the rotating ionosphere, however, the convection system clearly is not driven solely by the rotating earth. (Note, also that the center of rotation of the convection does not coincide with the earth's rotational axis, but is displaced about 15° from the pole.) We are inclined to believe that the basic convective pattern is established by the earth's rotation but is modified and amplified by energy diverted in some manner (though apparently not by viscous drag nor by line breaking and reconnection as these processes have previously been described) from the solar wind flow.

The radially directed electric field in the tail (depicted in Figure 8) has rather important consequences regarding the entry of low energy (i.e., less than a few kilovolts) particles into the tail. Briefly, its effect is to exclude protons altogether and to draw in electrons along the evening side and energize them to several tens of kilovolts. This is easily understood qualitatively. (Quantitative details of the particle motion are the subject of Section IV.) The magnetic drifts of protons and electrons are directed from morning to evening and from evening to morning, respectively. On the

morning side of the tail these drifts are in the direction opposite the electrical force on the two types of particles; thus, electrons and protons which enter there are de-energized as they are convected away from the earth by the $\overline{E} \times \overline{B}$ drift and do not penetrate far into the tail. On the evening side the electric force on electrons and protons is in the same direction as their magnetic drifts; thus, they will be energized as the E x B drift carries them toward the earth. However, a proton's magnetic drift, being toward the surface, does not carry it into the tail; protons are, therefore, excluded here also. An electron's magnetic drift carries it further into the tail, and it gains energy as it goes. Thus, in the energy range from a few kilovolts to a few tens of kilovolts, the particle population of the tail is expected to consist primarily of electrons.

The electrons' drift through the tail constitutes an electric current in the dawn-to-evening direction, and will have a tendency to distend the lines of force and, so, lengthen the tail. This suggests that magnetically-drifting electrons, caught up from the solar wind and energized by the rotational convective field of the tail, are the principal agent establishing and controlling the length of the magnetosphere's tail. The fact that the magnetic drift speed of the electrons

will be greatest where the magnetic field is weakest and most sharply curved may provide a kind of positive feed back mechanism whereby their effective current automatically becomes sharply concentrated in a sheet in the equatorial plane. We have not investigated this concept quantitatively. We note, however, that it would be expected to provide a tail whose length increases with increasing intensity of the solar wind. It seems clear that the current causing the sharp reversal of the magnetic field in the tail is produced by magnetic drift of the contained particles rather than by an electric field, for the electric field on the dawn-side of the tail is not directed properly to produce the currents which are implied by the neutral sheet found there.

An observed phenomenon which may provide information about the configuration of magnetic lines of force is the occurrence of high latitude auroral arcs. We show in Section V that solar wind particles are electrostatically accelerated to auroral energies only on lines of force which close in the magnetosphere. If we extend this to say that even high latitude auroral arcs must occur on closed lines, then Davis's [1962] observations of polar cap aurorae and of their anti-correlation with K_p [Davis, 1963] can be interpreted to mean that in quiet times practically all lines of force are closed, but that increasing

solar wind intensity breaks the very high latitude lines. The non-conservative electric field associated with these time-variations of the magnetic field should be capable of changing particle energies by many kilovolts. We believe that this acceleration mechanism may have an importance, in generating energetic particles, comparable to the electrostatic mechanism which we have considered in our calculations (especially at times of magnetic storms).

A feature of our model which should be noted is that the surface of the magnetosphere is an equipotential surface. This feature occurs because the field lines which make up the magnetospheric surface come out from the earth adjacent to the neutral point line; thus they have a potential which is equal to that of the neutral point line. If there were interconnection of the magnetospheric lines of force with the interplanetary lines of force, the magnetospheric surface might depart from an equipotential surface.

We have neglected the effects of interconnection of the field lines with the interplanetary fields as far as their influence on calculations with our model is concerned, because they appear to be much less significant than probable temporal variations in the electric and magnetic fields. For instance,

the non-alignment between the earth's axis of rotation and its magnetic moment will cause the potential of the surface of the magnetosphere to change relative to the potentials in the auroral zone. The variation in the potentials caused by the change in the corotation field will cause the potential difference between the surface of the magnetosphere and the midnight auroral zone to change by about $\pm$ 17 kV. In addition, the fact that the angle between the earth's magnetic moment and the ecliptic plane varies from about 12° to nearly 35° during the course of a year probably will influence both the magnetic and electric fields. It should cause the neutral point line to change latitude by several degrees and may well cause some kind of a seasonal shift in the SD currents. Fairfield [1964] indicates that both the patterns and the intensities of the SD currents are functions of season and universal time as well as magnetic local time. Quantitative evaluations of such variations would allow one to incorporate them into a model such as this.

The important question of what causes the SD electric fields remains unanswered although it must be basic to a full understanding of magnetospheric phenomena. We believe the fields presented here, however, to be reasonable approximations to the real electric and magnetic fields which exist in the

region surrounding the earth, at least in light of present day knowledge. Using this model of the fields we next evaluate the adiabatic motion of particles in such fields.

IV. ADIABATIC THEORY USED

Motion of charged particles in a complex configuration of electric and magnetic fields can be studied most conveniently if it can be assumed that the motion is adiabatic. Then the specification of three constants of the motion,

1. Total Energy, $K = W + qV,$ (5)
2. Magnetic Moment, $\mu = \frac{W}{B},$ (6)
3. Integral Invariant, $J = \oint p_{\parallel} ds,$ (7)

will describe the motion of a whole class of particles; that is, those having the specified K, μ, and J. μ and J are only approximate constants of the motion, though K is rigorously conserved if the electric field is conservative. The integral invariant can be written

$$J = \sqrt{2m\mu} \oint \sqrt{B_m - B}\ ds \qquad (8)$$

where B_m is defined by $\mu = \frac{W}{B_m}$ and in this case, where the field lines are assumed to be equipotentials, B_m is the value of the field at the turning point of the particle's motion. So one is led to use

$$J' = J/\sqrt{2m\mu} = \oint \sqrt{B_m - B}\ ds \qquad (9)$$

as the third constant of the motion. The only variable in the integral is B so J' can be calculated simply if the fields are known. When one knows the fields, a specification of K, μ, and J' for a particle determines a surface on which the particle must be found. In addition, the kinetic energy, W, the mirror B value, B_m, the particle pitch angle, etc., can be calculated as a function of position on this surface.

Formally the process of determining the particle motion may be described in the following manner. First it is necessary to define a coordinate system which specifies the individual lines of force in the magnetic field. This can be conveniently taken to be the magnetic co-latitude, θ_o, and magnetic longitude, ϕ_o, of the intersection of a line of force with the earth's surface. (Longitude is measured from the earth-sun line and the dipole axis is taken as the polar axis, assumed in this model to be perpendicular to the ecliptic plane.) In such a coordinate system, J' can be written as

$$J' (\theta_o, \phi_o, B_m) . \qquad (10)$$

Now since K and μ are also constants of the motion and $K = \mu B_m + qV$, we see

$$B_m = \frac{K - qV}{\mu} \quad . \tag{11}$$

Thus we can substitute this expression for B_m into the above expression for J' to obtain

$$J' (\theta_o, \phi_o, V), \quad K = \text{const}, \quad \mu = \text{const}. \tag{12}$$

Note, however, that the functional dependence of J' on V will depend on the values of K and μ for the particle.

V is a known function of θ_o and ϕ_o; thus the above expression is equivalent to

$$J' (\theta_o, \phi_o), \quad K = \text{const}, \quad \mu = \text{const}. \tag{13}$$

So for each set of values for K and μ, one can draw contours of constant J' in θ_o, ϕ_o space and in this way specify the magnetic lines of force on which the particle moves. Then other interesting quantities are given by

$$B_m = \frac{K - qV}{\mu} \tag{11}$$

$$W = \mu B_m \tag{14}$$

$$\sin \alpha = \sqrt{\frac{B}{B_m}} \quad \text{etc.} \tag{15}$$

The direction of drift along the constant J' surface is obtained from the expression for the average velocity of drift toward the new field line given by Northrop and Teller [1960] which, for static fields, reduces to

$$\langle \bar{v} \rangle = \frac{c}{q\,T\,B} \left(\bar{\nabla} J \times \bar{B} \right) \qquad (16)$$

where T is the latitudinal bounce period of the particle. The meaning of the other symbols is obvious.

In practice, particle parameters were determined in just this way. The integral defining J' was evaluated numerically on the University of Iowa IBM 7040 computer. Lines were selected at intervals of 1° for θ_o between 5° and 30° and at intervals of 30° for ϕ_o from 0° to 180°. Several extra lines were used around the neutral point line to determine the surface of the magnetosphere more accurately. Plots of J' vs B_m were made for each line. See Figures 9, 10, and 11. From the electric field in Figure 6 a table was made of the potential of the field lines for which J' had been calculated. Thus by choosing values for K and μ, equation (11) is used to find the value of B_m for particles on each field line. Then using the J' vs B_m curves the value of J' is determined for each field line. These values are then plotted on a θ_o, ϕ_o plot,

i.e., on the polar regions, and contours of constant J' can be drawn. Thus a set of plots of contours of constant J' are obtained for various pairs of values for K and μ (see Figures 12, 13, and 14).

To understand particle motions in terms of these curves two significant lines were added: first a curve on which the particle kinetic energy vanishes, i.e., W = 0 line. This line is found by observing that $W = 0 \Longrightarrow K = q\, V_b$ where V_b is the potential on this boundary curve. Since $W > 0$ and $W = q\,(V_b - V)$ it is seen that for $q > 0$, $V < V_b$, and for $q < 0$, $V > V_b$. Thus positive particles are confined to the low potential side of the surface where $V = V_b$ and negative particles are confined to the high potential side of this same surface. Note that this bounding surface depends only on the chosen K, i.e., the total energy of the particles considered.

The second curve of interest is a contour defined by $B_m = 0.5$ gauss. This is the line on which particles of the chosen K and μ will mirror approximately at the surface of the earth. If V_p is the potential of a particle when its $B_m = 0.5$ gauss then we find

$$q\, V_p = K - \mu\,(0.5)\,. \qquad (17)$$

u is in keV/gauss, K is in keV, V_p is in kV, and q = +1 for protons, -1 for electrons. Thus the contour where B_m = 0.5 gauss corresponds to the equipotential curve where $V = V_p$. From this it can easily be seen that particles of a given μ, K, and J' will precipitate when the contour of constant J' crosses the B_m = 0.5 gauss contour, which will hereafter be called the precipitation contour. The precipitation contours for electrons and protons are labeled "electron precip" and "proton precip", respectively, in Figures 12, 13, and 14. Note that the precipitation contour depends on both K and μ.

V. PRECIPITATION OF SOLAR WIND PARTICLES

In the preceding section it has been shown that from the adiabatic invariants and the configuration of the field one can deduce the motion of charged particles. In what follows this motion will be evaluated for particles starting in the solar wind with an energy less than ~ 1 keV. It will be assumed that these particles become trapped on the lines of force which make up the surface of the magnetosphere. Then, once the particle is in a trapped orbit, it will drift through the magnetosphere on a surface of constant J'. Conservation of K and μ will require that the particle kinetic energy and its mirror B change as the particle drifts. It will be shown that electrons moving in this manner will be energized to energies between 1 and 40 keV and precipitated during magnetic nighttime in a relatively narrow zone defined by the configuration of the fields. Protons will be energized to similar energies and precipitated during the period starting at noon, local magnetic time, and continuing through the night in a narrow region to the south of the region where electrons are precipitated.

Since the lines of force which make up the surface of our model all come out from the earth adjacent to the neutral point line, the surface of the model magnetosphere is an

equipotential surface. The potential was arbitrarily chosen to be 0 at $\Theta = 30°$ on the dusk meridian in the electric field used. This made the potential of the surface +18. (Probably a more logical choice would have been to make the surface of the magnetosphere have zero potential.) At any rate, in our model, solar wind particles ($W < \sim 1$ keV assumed) will have a total energy, $K = \pm 18 \pm 1$ keV, i.e., electrons have a total energy of ~ -17 to -18 keV and protons have a total energy of +18 to +19 keV. For the purposes of the following discussion this 1 keV difference is neglected, and all solar wind particles are assumed to have a total energy of 18 keV. Therefore, as was shown before, the electrons will be confined to lines of force with $V > 18$ kV, while the protons are confined to lines of force with $V < 18$ kV.

The potential plot shows that the 18 kV equipotential corresponds roughly with the auroral zone. Figures 12, 13, and 14 show that electron precipitation will occur primarily during magnetic local nighttime since the precipitation lines for electrons are confined to this region. Furthermore, there will be a gradual decrease in precipitation as one goes northward with a maximum latitude beyond which trapping can no longer occur. In this model, as Figures 12 to 14 show, the electron precipitation

will occur between 1800 and 2400 MLT (magnetic local time) in a zone between 12° and 20° co-latitude, while after midnight the precipitation zone should move southward about 5° so that by 0300 it is between 17° and 25°. Precipitation should end before dawn since the potential begins to decrease as one progresses around a J' = const curve.

A similar analysis for protons shows the precipitation region to be primarily between 1200 and ~ 1800, but a thin band of proton precipitation extends around as far as the electron precipitation region. Protons precipitate south of the electrons and will be bounded on the south during the nighttime by that J' = constant line which just fails to turn back toward noon in the daytime region. The precipitation patterns are shown roughly in Figure 15.

A characteristic of the particles which will tend to keep electrons, in particular, confined to a relatively narrow latitude range is their initial pitch angle distribution or what is equivalent, the initial distribution of their B_m. If one assumes that particles are initially trapped with an isotropic pitch angle distribution in a field of ~ 30 γ, it can be shown that 99% will mirror at B values less than ~ 1500 γ and 50% will mirror at B values less than ~ 120 γ.

This means that the most probable J' values lie between 0.5 and 8 (R_E gauss$^{1/2}$). A reasonable estimate appears to be that more than 90% of the incoming solar wind particles will have $0.5 \leq J' \leq 8\ R_E$ gauss$^{1/2}$ or that more than 50% of the incoming solar wind particles will have $0.5 \leq J' \leq 3$. This can be seen (Figures 12, 13, and 14) to preferentially confine electrons to a small latitude zone near the W = 0 line but will not have as much of a confining effect on protons, especially in the afternoon.

As observed by satellite borne detectors, particles moving in the manner described should have several striking features. Perhaps the most striking will be the boundary between the proton region and the electron region. In the discussion above the initial kinetic energy of the protons and electrons was ignored, and thus a line boundary was predicted. Actually the boundary will be a region in which very low-energy electrons and protons are found. The width of the boundary should correspond to a potential difference equal to the sum of the maximum proton kinetic energy and maximum electron kinetic energy as the particles enter the magnetosphere. This would appear to be a few kilovolts for solar wind particles. The corresponding width of the boundary is roughly 100 km near local midnight, and 200 km near local noon. The boundary

should reach its greatest width just before dusk or just after dawn, where the electric field is weakest and therefore the equipotential lines are farthest apart. Here it may be as much as 500 km across. At any rate one should observe a general anticorrelation between 1-40 keV electrons and 1-40 keV protons, i.e.,

$$\left.\frac{j\ (W_e < 40\ \text{keV})}{j\ (W_p < 40\ \text{keV})}\right|_{\text{NORTH of boundary}} \gg \left.\frac{j\ (W_e < 40\ \text{keV})}{j\ (W_p < 40\ \text{keV})}\right|_{\text{SOUTH of boundary}}$$

Another striking feature of the theory is the spectral change expected as one crosses the boundary. It seems reasonable to assume that the particles from the solar wind are the most abundant particles in the region where they are allowed. To the south of this region are found more durably-trapped particles which (at least in the case of electrons) are known to have a harder spectrum. Then the electron spectrum between 1 and 100 keV should be much softer north of the boundary than south of it, i.e.,

$$\left.\frac{j\ (W_e < 40\ \text{keV})}{j\ (W_e > 40\ \text{keV})}\right|_{\text{NORTH}} > \left.\frac{j\ (W_e < 40\ \text{keV})}{j\ (W_e > 40\ \text{keV})}\right|_{\text{SOUTH}}$$

The solar wind particles cannot be accelerated to energies greater than ~ 40 keV by the fields assumed in this model.

An opposite effect might be expected for protons but for the fact that the intensity of the high energy, more durably trapped protons may decrease rapidly with increasing latitude in this region.

It is interesting to note that this theory predicts that all particles whose kinetic energy at the surface of the magnetosphere is negligible, when observed within the magnetosphere will have a kinetic energy equal to the potential difference between the magnetospheric surface and the field line on which the particle is observed. This means that equipotential surfaces will appear as surfaces on which particles of a definite energy are observed. These surfaces at auroral latitudes are roughly aligned with the contours of constant magnetic latitude. However, they do deviate from such contours in a fixed manner. This would appear to earthbound observers as a local time variation in the energy of precipitated particles. Satellite observations should indicate a change in particle energy proportional to the change in the potential difference between the field line on which the particles are observed and that of the surface of the magnetosphere.

A consideration of the electric fields used in this model shows that particles observed near the surface of the

earth at a given latitude will have energies which are a few keV during the early evening and get progressively larger at later times around to a few hours after midnight. The maximum energy attainable is about 35 keV.

The simple picture derived from our calculation is modified by several phenomena which we have not considered in detail. For one thing the incoming particles (i.e., particles in the transition region surrounding the magnetosphere) are observed to have energies up to at least several tens of kilovolts. These particles will be found to have energies several tens of kilovolts different from those particles whose energies were small on the surface. If the energy spectrum outside the magnetosphere is sufficiently soft these higher energy particles will not contribute significantly to the fluxes. Another factor is the presence of nonconservative electric fields due to $\frac{\partial \vec{B}}{\partial t}$. The particle energization caused by such fields is not considered in this theory, and only if such fields produce energy changes that are negligible should the theory give accurate predictions. Actually, there probably are nonconservative fields (for example that due to the wobble of the earth's magnetic axis) which can cause energy changes of the same order as those caused by the

conservative fields, and these will probably give rise to a temporal and spatial modulation of the particle patterns. Such fields may also be able to drive particles from the auroral regions into the radiation belts. A final factor which we mention, although we feel it is probably negligible, is that of particles originating within the magnetosphere instead of on its surface. If such particles have low energy ($W < \sim 1$ keV) when they become trapped initially they will be confined to one side of the equipotential surface on which they originate. The processes causing particles to originate in the magnetosphere all appear to be weak and incapable of producing the intense auroral fluxes, e.g., acceleration of ionospheric particles, nuclear decay, ionization of neutral atoms, etc.

In short, the fact that one observes a spectrum of particle energies rather than a monoenergetic beam at a given point in the auroral zone or at higher latitudes does not imply that the auroral process we have described does not take place, but that other processes which we have not considered in detail also contribute.

In summary, our model provides the following description of auroral processes:

1. Auroral particles originate in the solar wind with energies $< \sim 1$ keV.

2. They are trapped near the surface of the magnetosphere with $0.5 \lesssim J' \lesssim 5.0$ R_E gauss$^{1/2}$ and as they drift along surfaces of constant J' their energies are increased by the electrostatic field to 1 to 35 keV. They will not remain in trapped orbits (unless carried into them by nonconservative electric fields, a process which we have not considered) but will either precipitate into the atmosphere and be absorbed, or will drift back out of the magnetosphere again.

3. There will be a definite boundary between the region where solar wind electrons may be found and the region where solar wind protons may be found, the protons confined south of the electrons. The width of this boundary should be 100-500 km. The maximum widths should occur during the day, especially near the dawn-dusk meridian and the minimum widths should occur near midnight. The location of this boundary should be in the region of auroral activity.

4. Electron spectra should be harder south of the boundary than north of it.

5. Electron precipitation will occur primarily in a narrow range of latitudes on the night-side of the earth. Protons will be precipitated over a large area in the afternoon and in a narrow region south of the electrons throughout the night.

6. A fairly sharp boundary of the afternoon proton precipitation should occur at the magnetic noon meridian; no proton precipitation will occur in late morning hours.

VI. COMPARISON WITH EXPERIMENT

Although there have been many experimental studies of auroral phenomena, there have been relatively few measurements made of the low energy particles (1-20 keV) which are apparently the major source of energy for auroral phenomena [McIlwain, 1960]. It is the measurement of these particles which can be compared directly with our predictions.

The first measurements of these particles were apparently those of McIlwain. On two rocket flights into active auroras he detected intense fluxes of low energy electrons $j\ (W < 30\ \text{keV}) \sim 10^9$ electrons $(\text{cm}^2\ \text{sec sterad})^{-1}$. The proton fluxes in a similar energy range were at least a factor of 10^3 less intense. On one flight the electron spectrum appeared to be nearly monoenergetic at 6 keV. This is precisely what would be expected if the precipitation of solar wind electrons were caused by an electrostatic field. On his other flight, McIlwain reported an exponential spectrum with an e-folding energy of 5 keV, although he points out that the real spectrum could have been significantly different from this. He did find that most of the energy flux observed was due to electrons with energies of less than 40 keV.

McIlwain's measurements show that the particles associated with an auroral event are consistent with the predictions of our model. His two rocket flights, however, give no information on the spatial distribution of such particles. More recent satellite studies of these low energy particles by the Lockheed group [Sharp et al., 1964; Meyerott, 1964] give significant information about latitudinal and magnetic local time variations. These studies were made on five days of late October and early November 1963 with a satellite in a low altitude polar orbit. They indicate that proton precipitation does occur in the afternoon and during the night but is conspicuously absent in the late morning hours. (The times when this satellite passed through auroral latitudes were approximately 2200 to 0400 at night and 1000 to 1600 during the day.) In addition, these observations seem to indicate that the nighttime proton precipitation occurs at a lower latitude and over a smaller range of latitudes than the daytime precipitation. The nighttime proton precipitation appears to be somewhat more extensive than that predicted by our model. Such an effect could be explained by a minor modification of the electric potential system. If the 0 kV and -5 kV equipotential lines closed around the maximum of the potential system

instead of turning southward in the afternoon (see Figure 6), then many protons would drift around to the night side and occupy a wider band of latitudes instead of precipitating in the afternoon.

Sharp et al. [1964] find precipitation of electrons on both the day and night sides of the auroral zone. The daytime events have fluxes which are less intense and have a noticeably harder spectrum than the nighttime events. Daytime precipitation of electrons (at least before noon) is not predicted by our model, but the fact that the spectrum is harder and the events less intense may be an indication that these particles come from a different source. It may also be significant that these morning events occur on lines of force on which outer zone electrons ($W \gtrsim 40$ keV) are generally present whereas at least the northern part of the nighttime encounters are above the outer zone cutoff. One may then say that it is outer zone electrons which are observed to precipitate in late morning rather than electrons coming directly from the solar wind.

Further indications that these morning electrons are actually of different origin than those which are observed to precipitate at night are evident in the data of Fritz and

Gurnett [1965]. They observed no occurrences of low energy electron fluxes (W > 10 keV) greater than 2.5×10^7 particles $(cm^2 \text{ sec sterad})^{-1}$ during the daytime using nearly a year of Injun III data. This is an indication that the morning fluxes observed by the Lockheed group were actually smaller fluxes of more energetic particles, while the nighttime events were due to true auroral particles.

In Figure 16 the data of Fritz and Gurnett are superimposed on our predicted precipitation regions. We feel that the shape of the precipitation region is in reasonable agreement with the predictions based on our model. The fact that they find events at lower latitudes than we predict is partly due to the fact that the neutral point in our model should be at a few degrees lower latitude and therefore at a lower potential thus making the boundary farther south. The shape of the precipitation region is sensitive also to the choice of electric field. Rough calculations show that temporal changes in the electric field of the SD current system and in the co-rotation electric field (due to the wobble of the dipole axis) can shift the whole pattern of precipitation contours in our model by as much as 10 degrees of latitude. Thus one should not attach too much significance to the fact that particles

are observed to precipitate south of the region where the model predicts. We feel that the same methods applied to a model which included the time behavior of the electric field would reproduce the observed precipitation region with a high degree of accuracy.

We should probably point out that Fritz and Gurnett carried out an extensive frequency-of-occurrence analysis to show that the day-night asymmetry as well as the latitudinal dependence is real and not due to biased satellite sampling. In addition their determinations of electron spectra between 10 and 40 keV show nearly discontinuous softening as the satellite moves northward out of the outer zone.

Observations of the hydrogen aurora show that in the evening it generally occurs south of the region where atmospheric emissions (e.g., O, N_2^+, etc.), caused by electron bombardment, occur [see Rees et al., 1961]. It shows a diurnal variation moving to progressively lower latitudes during the pre-midnight hours. It is reported that the band of hydrogen light emission, which may cover one to ~ fifteen degrees of latitude, is often sharply separated from the brighter electron aurora to the north by a dark emissionless band [Galperin, 1963; Omholt et al., 1962]. The hydrogen emissions are generally

attributed to recombination of ionospheric electrons with protons stopped in the atmosphere. These observations obviously fit well with our theory since we do expect protons to precipitate south of the electron precipitation region during the nighttime. The dark emissionless band separating electron and hydrogen auroras is, by our theory, the W=0 line, that is, the surface within the magnetosphere whose potential is equal to that of the outer boundary of the magnetosphere.

Despite the rather striking agreements with predictions of the theory, we must point out that we do not predict an advance of the hydrogen aurorae to the north of the electrons after midnight--a feature which is frequently reported.

Finally, it is interesting to note that the high latitude boundary of the trapped particles in the outer zone as reported by various experimenters [O'Brien, 1963; McDiarmid and Burrows, 1964; Frank, Van Allen, and Craven, 1964] corresponds fairly well with the W=0 line of our model, i.e., with the low latitude boundary of the solar wind electrons. This may be an indication that the W=0 line mapped into the equatorial plane corresponds to the inner edge of the current sheet in the tail, since, as noted in Section II, energetic particles are not likely to be durably trapped on lines of force which penetrate the current sheet.

In general, experimental data seem to fit the predictions of our model very well. There are several deviations which indicate that at least in some regions of the magnetosphere there are processes taking place which we have not taken into account. Since we have not attempted to treat the electrons with $-18 < K < 500$ keV or protons with $18 < K < 500$ keV, a population which includes a large number of the particles trapped in the radiation belts, we cannot expect to have a complete picture. Furthermore, it is clear that there are significant time dependent components of the fields which we have also neglected. There are also phenomena depending on the stability of the distribution of plasma in the magnetosphere which are probably important in the total picture.

VII. COMPARISON WITH PREVIOUS MODELS

As was mentioned earlier, individual ingredients of this model were present in earlier models. These ingredients were a distorted dipole magnetic field and an electric field. Hones [1963] calculated magnetic field line configurations and convective motions of trapped particles in a distorted magnetic field taking into account only the electric field produced by the earth's rotation. Dessler and Juday [1965] have considered an extremely distorted model in their proposal of a magnetospheric tail many astronomical units long. Axford and Hines [1961] introduced the idea of internal convection (i.e., electric fields) driven by the solar wind. They did not, however, calculate particle motions in quantitative detail. Maeda [1964] and Hones [1965] have calculated particle paths in a dipole magnetic field and an electric field derived from the S_q currents. (Such calculations presumably give results which apply to motion on the low latitude magnetic field lines.) The present model combines the effects due to the distortion of the dipole magnetic field (both by the external pressure of the solar wind and by the newly-detected current sheet) with those due to a carefully derived representation of the electric field. This model provides what we believe

to be realistic explanations of many auroral processes. Dessler and Juday [1965, p. 63] objected to models such as this stating that the "primary difficulty with neutral point theories is explaining the occurrence of nighttime aurora." Their objection to models such as that of Axford and Hines is that it fails to predict an auroral "zone", i.e., does not confine auroral phenomena to a small range of latitudes. We have shown in this study that both these objections can be overcome. We do have a neutral point theory which predicts nighttime aurora and confines it to a relatively narrow latitudinal zone. Furthermore, it should be pointed out that this is accomplished with the neutral point line not at auroral zone latitudes but at a co-latitude of $\sim 10^{\circ}$, its location in theoretical models of the magnetosphere such as Mead's [1964].

A basic difference between this model and that of Axford and Hines is our reliance upon reasonably well founded electrostatic fields to produce acceleration and precipitation of auroral particles while Axford and Hines called upon convected turbulence to produce the auroral phenomena. Presumably one still must invoke turbulence or instability to explain the small scale details of precipitation patterns and auroral emissions.

VIII. CONCLUSIONS

We have found that calculations of adiabatic motion of charged particles in a model which incorporates reasonable representations of the static electric and magnetic fields surrounding the earth provide predictions of auroral phenomena which are consistent with observations. Thus, our study confirms the applicability of adiabatic theory to calculations of particle motions, even in the distant regions of the magnetosphere. We regard this confirmation as a particularly important result of our work. For, although only static fields have been considered here, the general applicability of adiabatic theory to time-varying fields [Northrop and Teller, 1960] implies that a wide range of phenomena attributable to the magnetospheric tail may be studied using the adiabatic approximation.

The general pattern of the electric potential system (and thus of the convective motions of low-energy plasma) in the magnetosphere appears to be established by the earth's rotation, but energy is added to this basic rotational convection pattern in some manner by the solar wind. The electric fields are such as to prohibit entry of solar wind protons into the tail of the magnetosphere while permitting

entry and subsequent energization of solar-wind electrons along the evening-side of the tail. The electrons, drifting from evening to dawn through the magnetosphere, constitute a current which establishes and controls the length of the tail.

The majority of the low energy particles found in auroral regions originate in the solar wind with a relatively small energy ($< \sim 1$ keV). These particles become temporarily trapped on the surface of the magnetosphere. As they bounce back and forth they drift longitudinally due to both the electric field and the inhomogeneities in the magnetic field. The particles are energized as their magnetic drifts carry them along in the direction of the electric force. As they attain energies in the range of 1 to 35 keV, while conserving their magnetic moment, they are continually driven to mirror at larger B values. Many of the particles will actually be driven down so that they mirror in the atmosphere and are lost. If a particle reaches its maximum energy without precipitating it will begin losing energy again and will drift back out of the magnetosphere (alternatively, particles might be driven by nonconservative electric fields to lines of force on which they will be stably trapped).

Electrons which precipitate will do so north of a line corresponding to the intersection of an equipotential surface with the surface of the earth. The potential of this surface is equal to that of the magnetospheric surface. The protons will precipitate south of this same line. Electrons will precipitate almost completely during the nighttime in a band which presumably corresponds to the auroral zone. The protons will precipitate over a widespread area in the afternoon and over a very narrow band just south of the electron precipitation region during the night.

ACKNOWLEDGEMENTS

The authors are pleased to acknowledge several stimulating and helpful conversations regarding the subject of this report with Dr. W. I. Axford, Dr. S.-I. Akasofu, and Dr. J. A. Fejer.

REFERENCES

Axford, W. I., Viscous interaction between the solar wind and the earth's magnetosphere, Planet. Space Sci., 12, 45-53, 1964.

Axford, W. I., and C. O. Hines, A unifying theory of high-latitude geophysical phenomena and geomagnetic storms, Can. J. Phys., 39, 1433-1464, 1961.

Axford, W. I., H. E. Petschek, and G. L. Siscoe, The tail of the magnetosphere, Avco Everett Research Report No. 190, August 1964.

Cahill, L. J., Jr., Preliminary results of magnetic field measurements in the tail of the geomagnetic cavity I. G. Bulletin 79, 1964.

Cahill, L. J., Jr., and P. G. Amazeen, The boundary of the geomagnetic field, J. Geophys. Res., 68, 1835-1843, 1963.

Chapman, S., The Earth's Magnetism, Methuen and Co., Ltd., London, 1951.

Chapman, S., and J. Bartels, Geomagnetism, Vol. I, Clarendon Press., Oxford 1951.

Davis, T. N., The morphology of the auroral displays of 1957-1958. 2. Detail analyses of Alaska data and analyses of high-latitude data, J. Geophys. Res., 67, 75-110, 1962.

Davis, T. N., Negative correlation between polar cap visual aurora and magnetic activity, J. Geophys. Res., 68, 4447-4453, 1963.

Dessler, A. J., and R. D. Juday, Configuration of auroral radiation in space, Planet. Space Sci., 13, 63-72, 1965.

Fairfield, D. H., Ionospheric current patterns in high latitudes, J. Geophys. Res., 68, 3589-3602, 1963.

Fairfield, D. H., A study of high latitude ionospheric current patterns--with emphasis on the 12th hour U.T., Penn State Ionospheric Research Report No. 217, 1964.

Fejer, J. A., Semidiurnal currents and electron drifts in the ionosphere, J. Atm. Terr. Phys., 4, 184-203, 1953.

Frank, L. A., J. A. Van Allen, and J. D. Craven, Large diurnal variations of geomagnetically trapped and of precipitated electrons observed at low altitudes, J. Geophys. Res., 69, 3155-3167, 1964.

Fritz, T. A., and D. A. Gurnett, Diurnal and latitude effects observed for 10 keV electrons at low satellite altitudes, University of Iowa Research Report 65-3, February 1965.

Gal'perin, Yu. I., Proton bombardment in aurora, Planet. Space Sci., 10, 187-193, 1963.

Heppner, J. P., N. F. Ness, C. S. Scearce, and T. L. Skillman, Explorer 10 magnetic field measurements, J. Geophys. Res., 68, 1-46, 1963.

Hones, E. W., Jr., Motions of charged particles trapped in the earth's magnetosphere, J. Geophys. Res., 68, 1209-1219, 1963.

Hones, E. W., Jr., Adiabatic motions of charged particles in a dipole model of the magnetosphere, University of Iowa Research Report 65-6, March 1965.

Levy, R. H., H. E. Petschek, and G. L. Siscoe, Aerodynamic aspects of the magnetospheric flow, Avco Everett Research Report No. 170, December 1963.

Maeda, H., Electric fields in the magnetosphere associated with the daily geomagnetic variations and their effect on trapped particles, J. Atm. Terr. Phys., 26, 1133, 1964.

McDiarmid, I. B., and J. R. Burrows, High-latitude boundary of the outer radiation zone at 1000 km, Canadian J. Phys., 42, 616-626, 1963.

McIlwain, C. E., Direct measurement of particles producing visible auroras, J. Geophys. Res., 65, 2727-2747, 1960.

Mead, G. D., Deformation of the geomagnetic field by the solar wind, J. Geophys. Res., 69, 1181-1195, 1964.

Meyerott, R. C., Input-output experiment, Semiannual Technical Summary Report for Period ending 30 September 1964, Lockheed Missiles and Space Co., Sunnyvale, California.

Ness, N. F., The earth's magnetic tail, Goddard Space Flight Center Report X 612-64-392 Revised Jan. 28, 1965.

Ness, N. F., C. S. Searce, and J. B. Seek, Initial results of IMP-2 magnetic field experiment, J. Geophys. Res., 69, 3531-3570, 1964.

Northrop, T. G., and E. Teller, Stability of the adiabatic motion of charged particles in the earth's field, Phys. Rev., 117, 215-225, 1960.

O'Brien, B. J., A large diurnal variation of the geomagnetically trapped radiation, J. Geophys. Res., 68, 989-995, 1963.

Omholt, A., W. Stoffregen, and H. Derblom, Hydrogen lines in auroral glow, J. Atmos. Terr. Phys., 24, 203-209, 1962.

Rees, M. H., A. E. Belon, and G. J. Romick, The systematic behavior of hydrogen emission in the aurora: I, Planet. Space Sci., 5, 87-91, 1961.

Sharp, R. D., J. E. Evans, R. G. Johnson, and J. B. Reagan, Measurement of total energy flux of electrons precipitating on auroral zones, to appear in Proceedings of 1964 Cospar Meeting, Florence.

Silsbee, H. C., and E. H. Vestine, Geomagnetic bays, their frequency and current systems, Terr. Mag. and Atmos. Elect., 47, 195-208, 1942.

Sugiura, M., and S. Chapman, The average morphology of geomagnetic storms with sudden commencements, Abh. Akad, Wiss. Göttingen, Math.-Phys., Kl. Sonderheft Nr. 4, 1960.

FIGURE CAPTIONS

Figure 1. The cross section of the model used for the magnetic field in the noon-midnight plane. The strength of the image dipole moment (μ_I), its distance (D_I) from the dipole of the earth μ_E, and the strength of the magnetic field caused by the current sheet were the parameters varied to fit magnetometer measurements of the real field. Numbers along anti-solar axis are radial distances in R_E.

Figure 2. Intersections of the magnetic lines of force with the geomagnetic equatorial plane. Points are labeled with the co-latitude of the field line at the surface of the earth. Most of the points shown represent lines which emanate from meridian planes spaced at intervals of 30° in longitude beginning at the noon meridian. Numbers along the axes are radial distances in R_E. View is from above North Pole.

Figure 3. Location on the earth's surface of the field lines which make up the magnetospheric tail.

Figure 4. Twelve month average of SD currents in the polar ionosphere derived from magnetic bays [after Silsbee and Vestine, 1942].

Figure 5. Potential system derived from current system in Figure 4 mapped on the geomagnetic polar regions. Each circle represents 5° co-latitude.

Figure 6. Potential system of Figure 5 corrected for charge separation caused by the rotation of the ionosphere with the earth. Equipotential curves are labeled in kilovolts.

Figure 7. Electric potentials of Figure 6 mapped into the equatorial plane viewed from above North Pole.

Figure 8. Equipotentials (kV) mapped into a plane perpendicular to the axis of the magnetospheric tail at a radial distance of 40 R_E. View is toward the sun from far behind the earth. Dashed lines connect points of intersection of the lines of force emanating from a constant co-latitude (θ_o) on the surface of the earth with the plane $x = -40\ R_E$. Numbers along these curves are the longitude of the field lines at the earth in degrees.

Figure 9. Plot of J' versus B_m for selected field lines which emanate from the surface of the earth within 1° of the noon meridian plane. Curves are labeled with the co-latitude of the field line at the surface of the earth.

Figure 10. Plot similar to Figure 9 for field lines emanating from dawn or dusk meridian plane.

Figure 11. Plot similar to Figure 9 for field lines emanating from midnight meridian plane.

Figure 12. Intersection of surfaces of constant J' with the surface of the earth for solar wind particles with $\mu = 50$ keV/gauss. ----- curves of constant J' for protons. — .. — .. — curves of constant J' for electrons. Labels on constant J' curves are in units of (R_E gauss$^{1/2}$). Arrows give direction of drift along constant J' curve.

Figure 13. Plot similar to Figure 12 for μ = 20 keV/gauss.

Figure 14. Plot similar to Figure 12 for μ = 5 keV/gauss.

Figure 15. Summary of regions where the assumed electrostatic fields will cause solar wind particles to precipitate.

Figure 16. Comparison of electron region with Injun III satellite observations. Black dots represent the approximate position at the surface of the earth of field lines on which intense fluxes ($\gtrsim 2.5 \times 10^7$ particles $(cm^2 \text{ sec sterad})^{-1}$) of low energy ($W \gtrsim 10$ keV) electrons were encountered. Singly crosshatched area is region where solar wind electrons are allowed in our model.

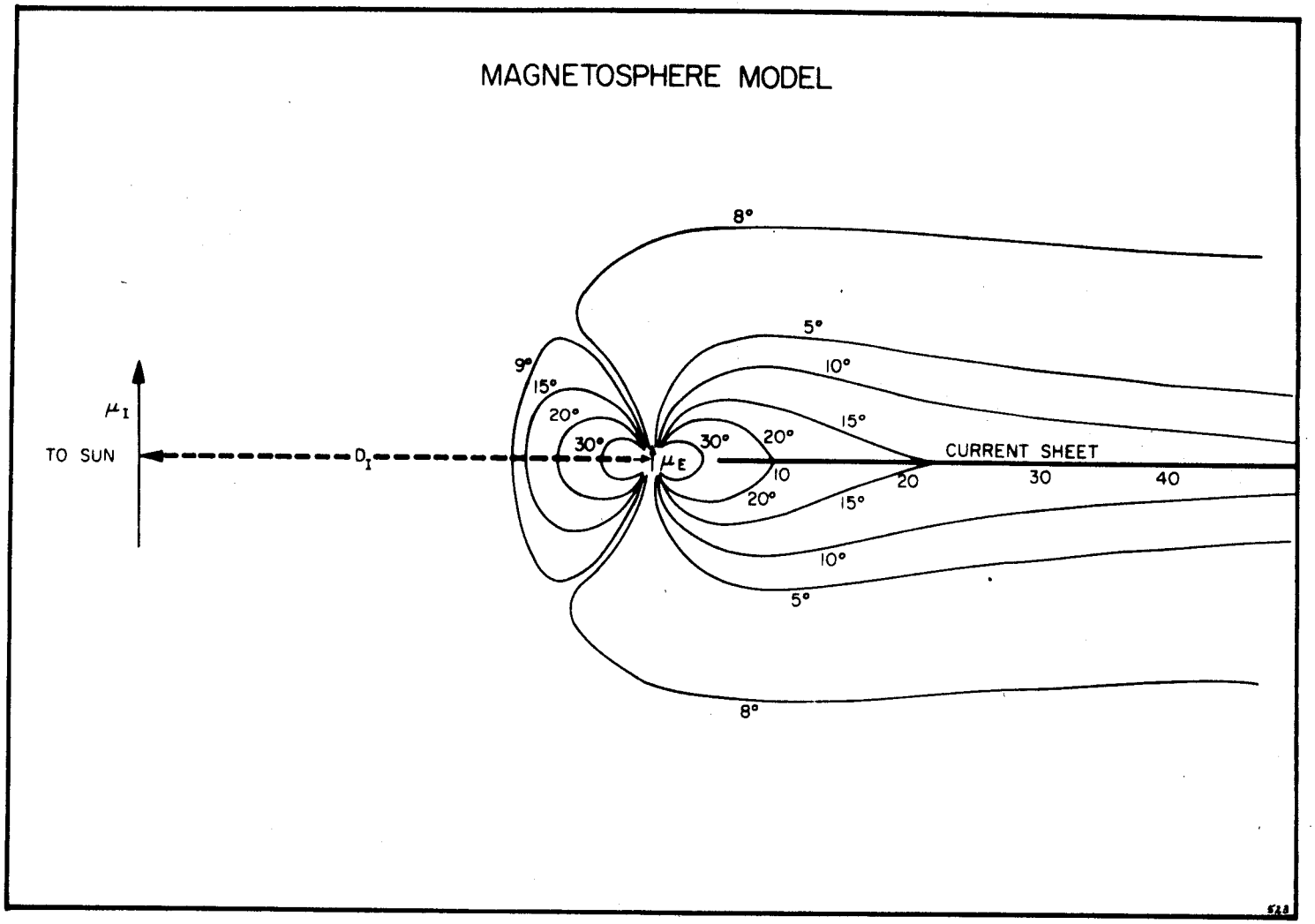
MAGNETOSPHERE MODEL
8°
5°
10°
15°
20°
30°
9°
15°
20°
30°
μ_I
TO SUN
D_I
μ_E
30°
20°
15°
CURRENT SHEET
10
20
30
40
20°
15°
10°
5°
8°

Figure 1

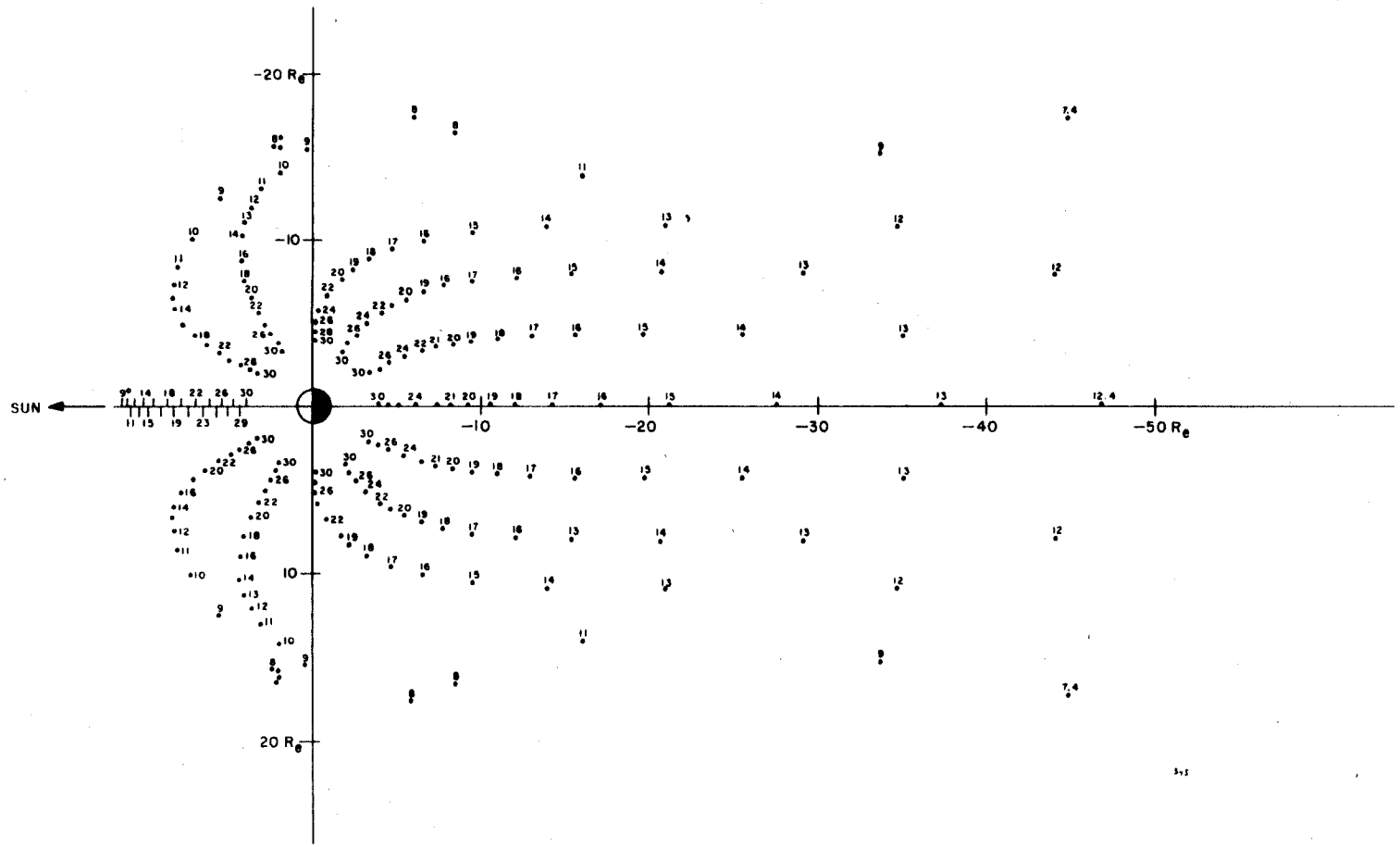

Figure 2

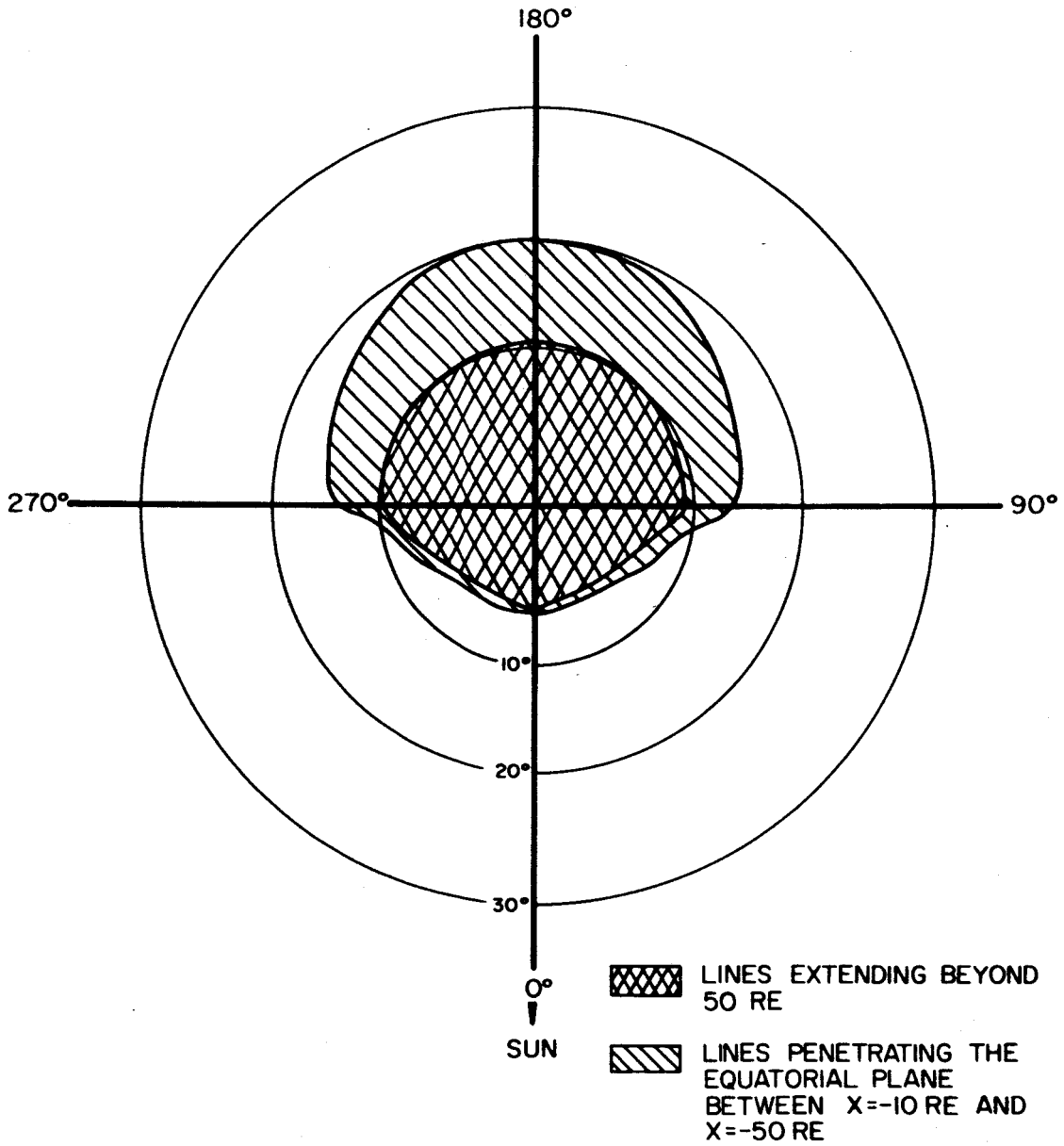
180°
270°
90°
10°
20°
30°
0°
SUN
LINES EXTENDING BEYOND 50 RE
LINES PENETRATING THE EQUATORIAL PLANE BETWEEN X=-10 RE AND X=-50 RE

Figure 3

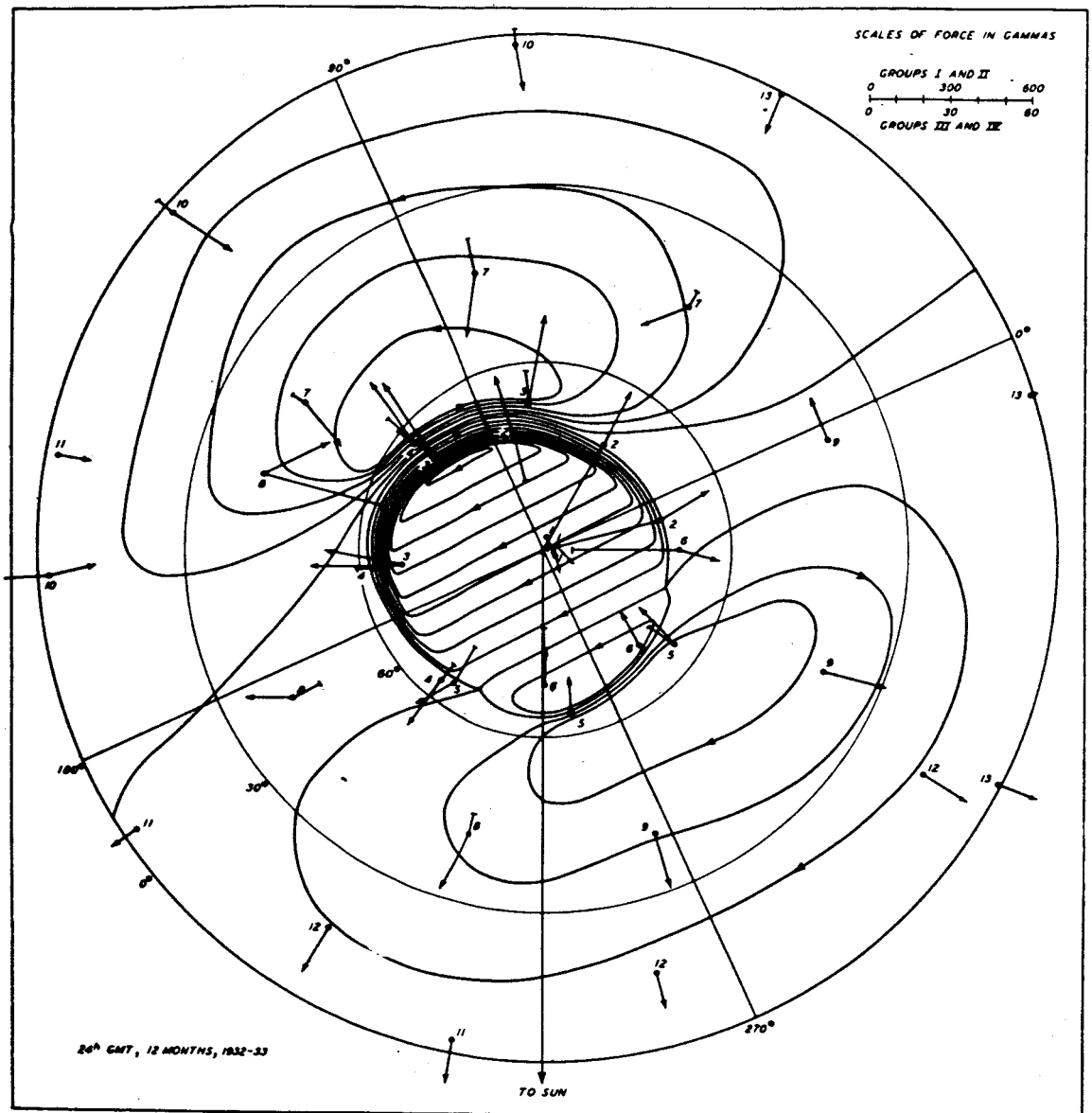

MEAN 3-HOUR DISTURBANCE-VECTORS OF MAGNETIC BAYS CENTERED AT 21h, 24h, AND 3h GMT (TENTATIVELY CORRECTED FOR INDUCED CURRENTS) AND CORRESPONDING AVERAGE ELECTRIC CURRENT-SYSTEM OF HEIGHT 150 KM, DERIVED FROM DATA OF FIGURE ; VIEW FROM ABOVE GEOMAGNETIC NORTH POLE

LEGEND

HORIZONTAL FORCE ——→ VERTICAL FORCE ——◁ (VERTICAL COMPONENT POSITIVE WHEN DRAWN OUTWARDS FROM GEOMAGNETIC NORTH POLE)
(50,000 AMPERES FLOW BETWEEN SUCCESSIVE CURRENT-LINES)

STATIONS

GROUPS I AND II		GROUPS III AND IV	
1 THULE	4 DICKSON	7 EBRO	10 MOGADISCIO
2 JULIANEHAAB	5 COLLEGE-FAIRBANKS	8 WATHEROO	11 ANTIPOLO
3 TROMSÖ	6 FORT RAE	9 TUCSON	12 APIA
			13 HUANCAYO

Ionospheric Current System taken from Silsbee and Vestine [1942].

FIGURE 4

POTENTIAL PLOT FROM RADIAL COMPONENT OF E FIELD

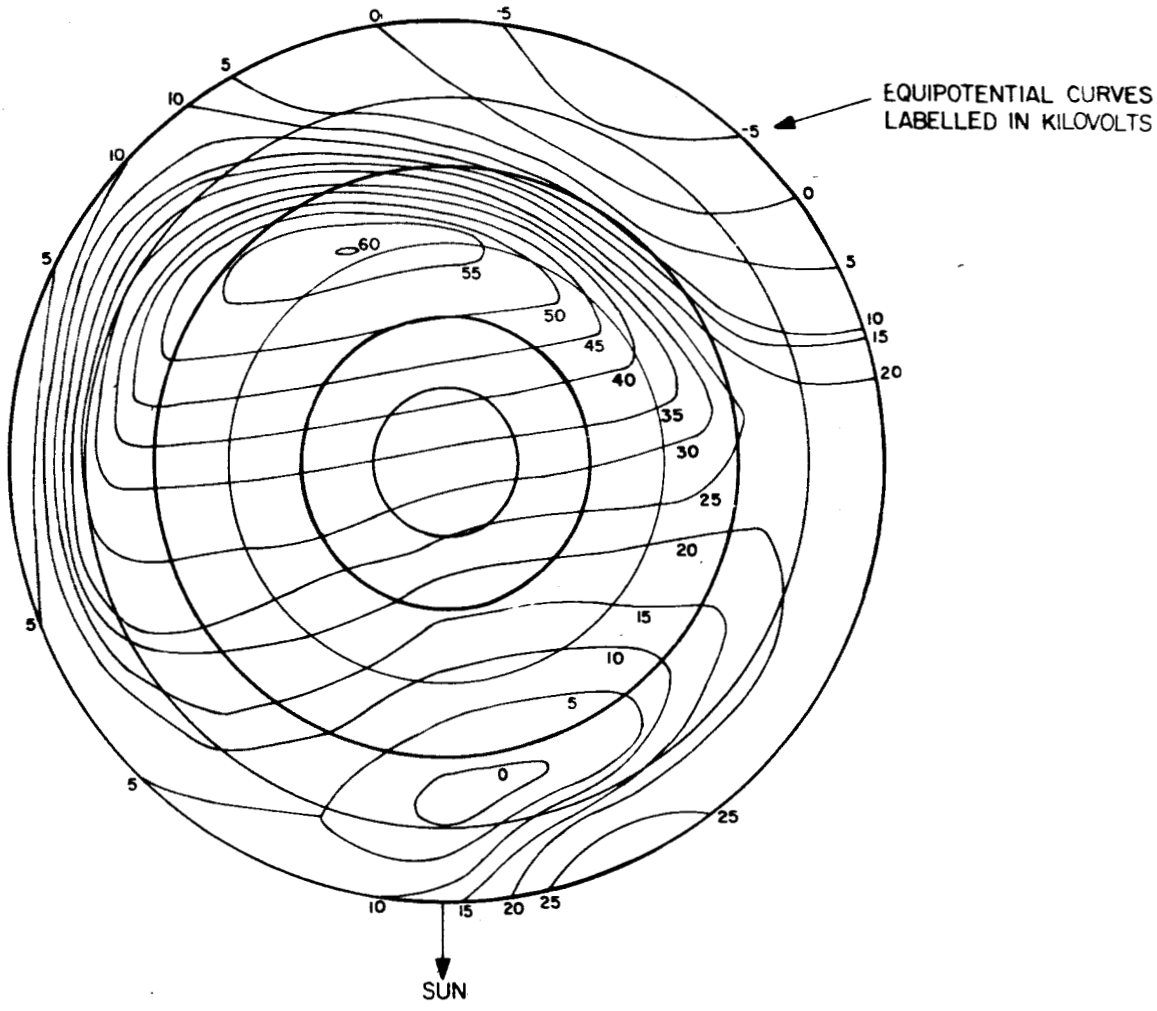

Figure 5

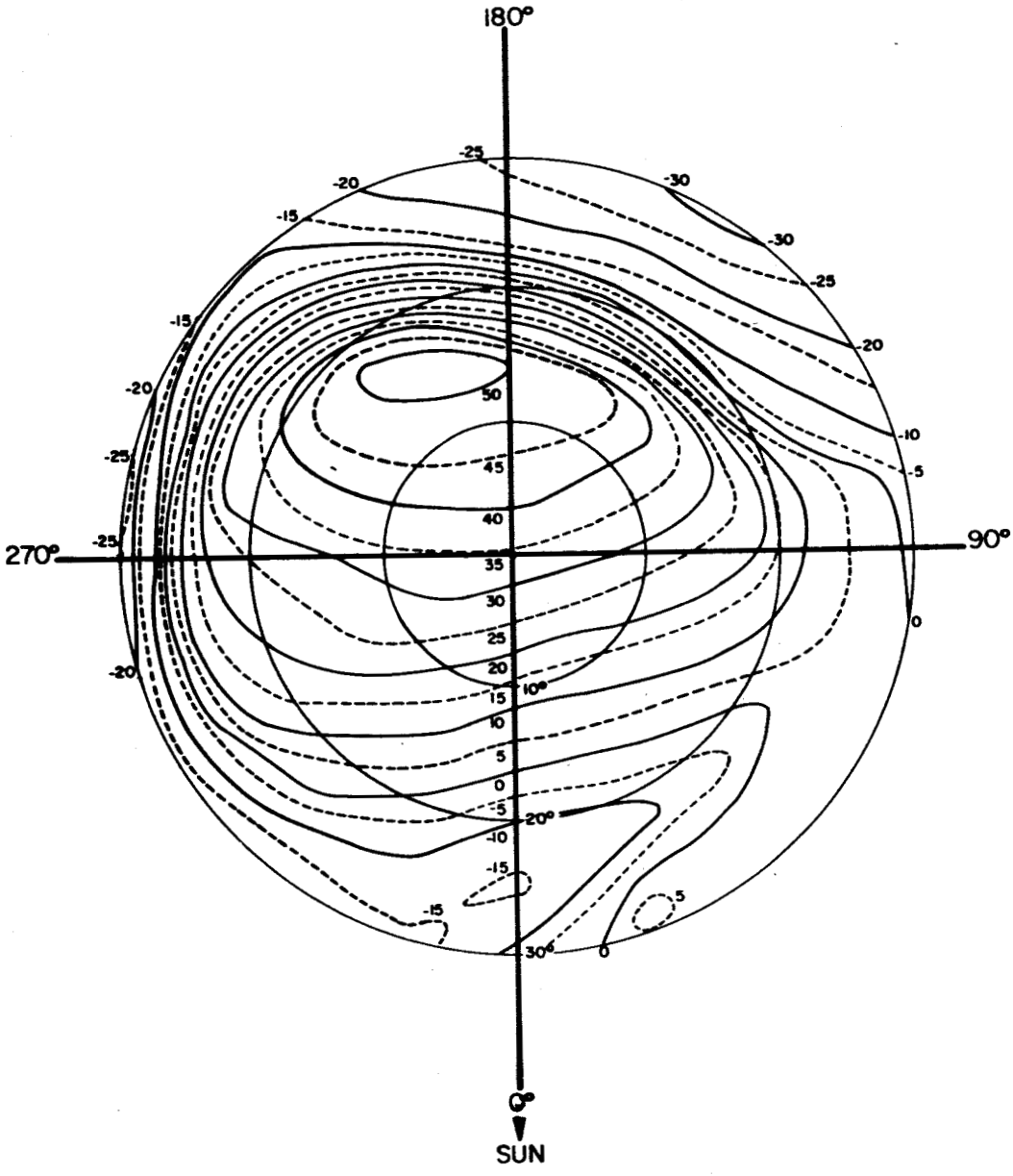
180°
270°
90°
0°
SUN
-25
-20
-15
-30
-10
-5
50
45
40
35
30
25
20
15
10
5
0
-5
-10
-15
10°
20°
30°

FIGURE 6

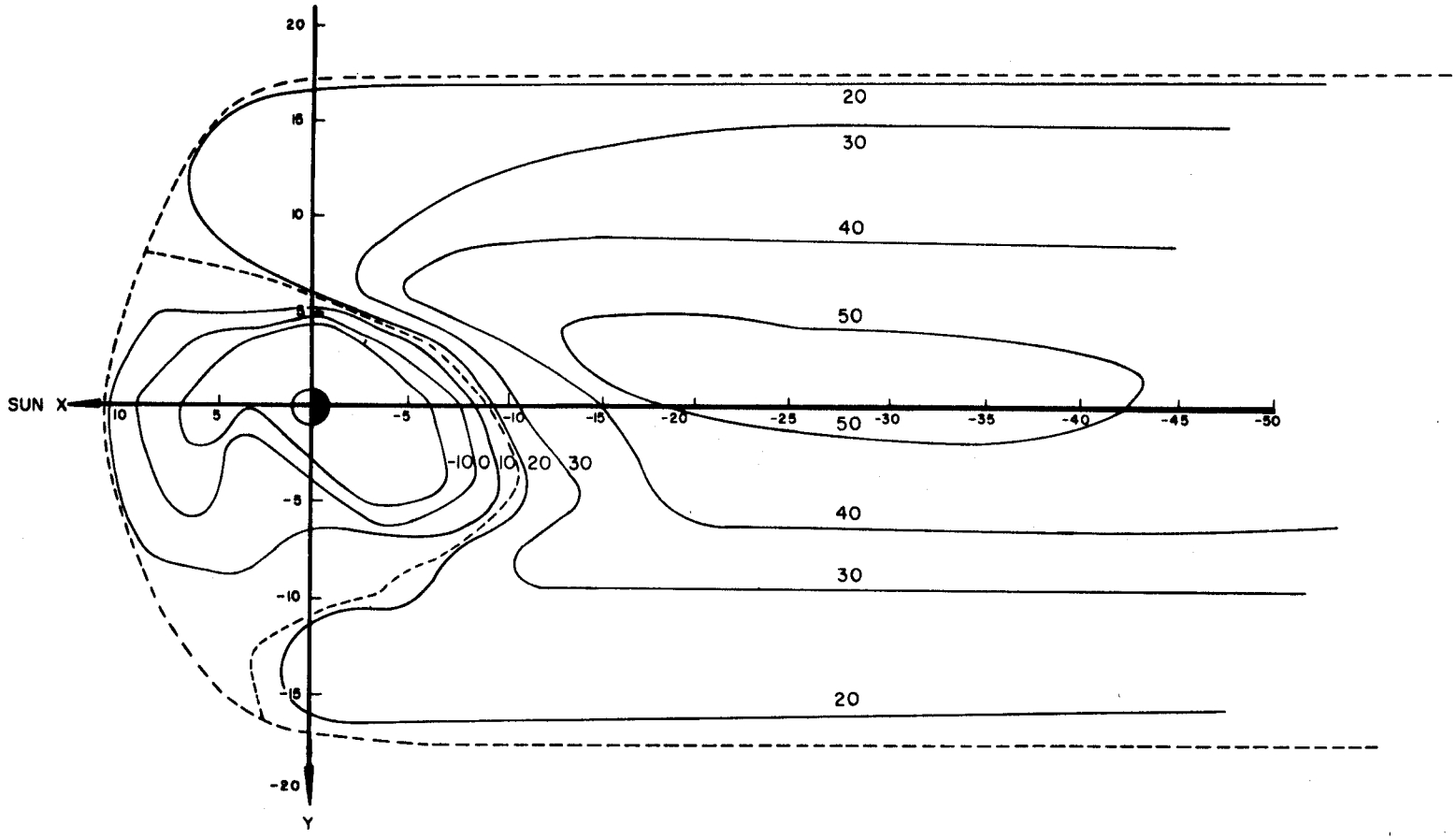

ELECTRIC POTENTIALS MAPPED INTO THE EQUATORIAL PLANE
(INCLUDES COROTATIONAL EFFECTS)

Figure 7

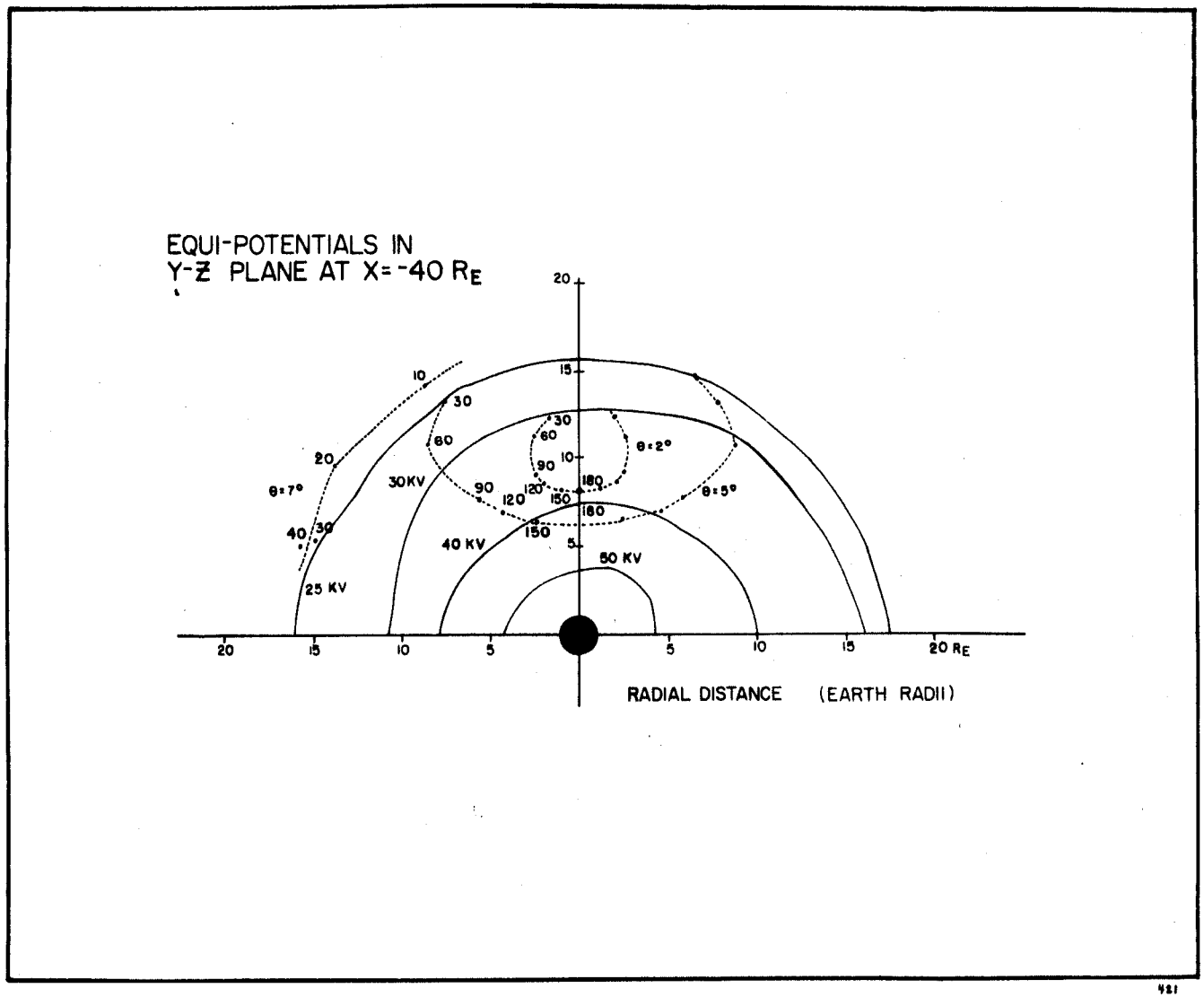
EQUI-POTENTIALS IN
Y-Z PLANE AT X=-40 RE
20
15
10
5
30
60
90
120
150
180
θ=7°
θ=2°
θ=5°
30KV
40 KV
50 KV
25 KV
40
20
20 RE
RADIAL DISTANCE (EARTH RADII)

Figure 6

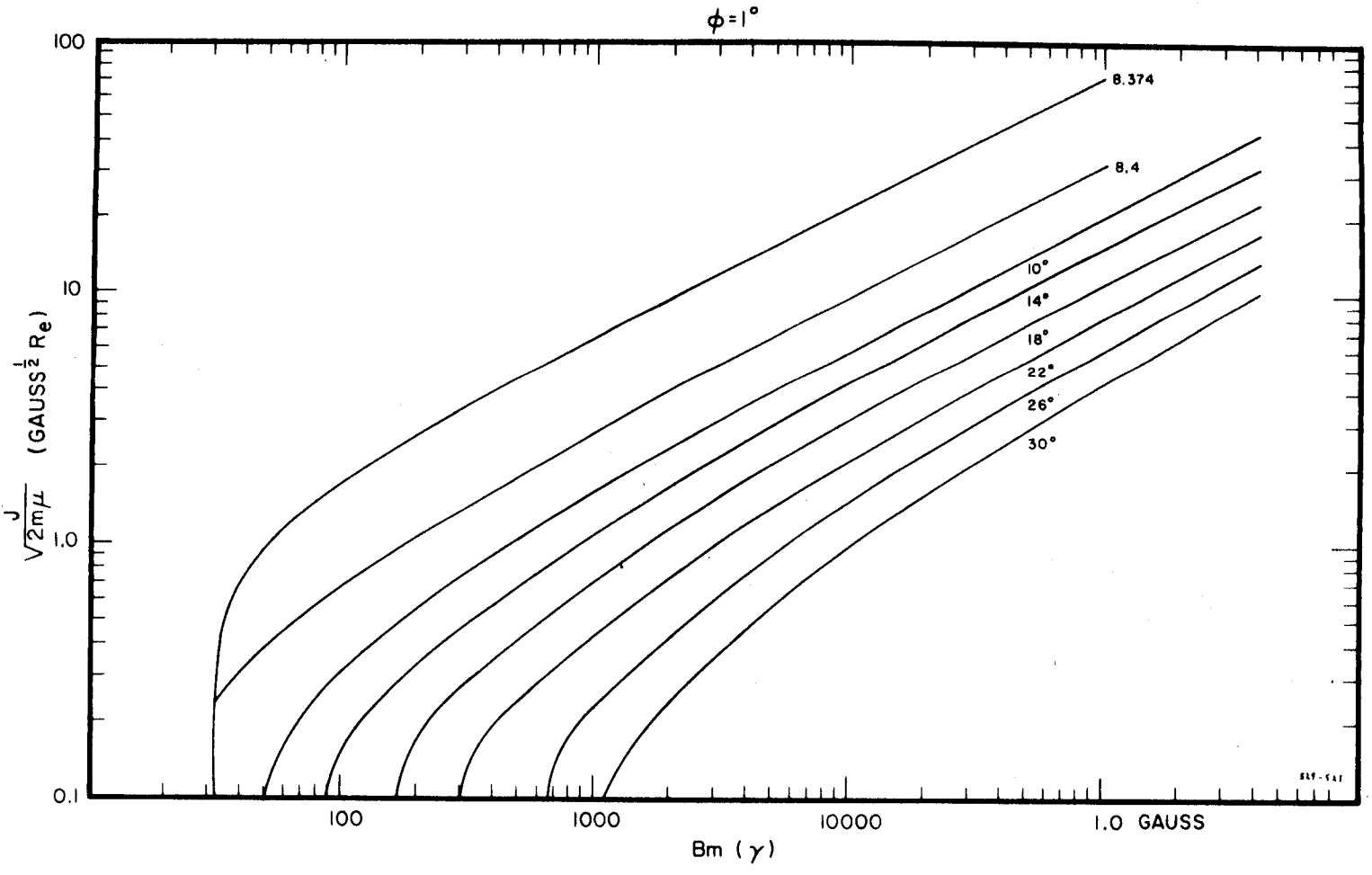
$\phi = 1°$
100
10
1.0
0.1
$\frac{J}{\sqrt{2m\mu}}$ (GAUSS$^{\frac{1}{2}}$ R_e)
8.374
8.4
10°
14°
18°
22°
26°
30°
100
1000
10000
1.0 GAUSS
Bm (γ)

Figure 9

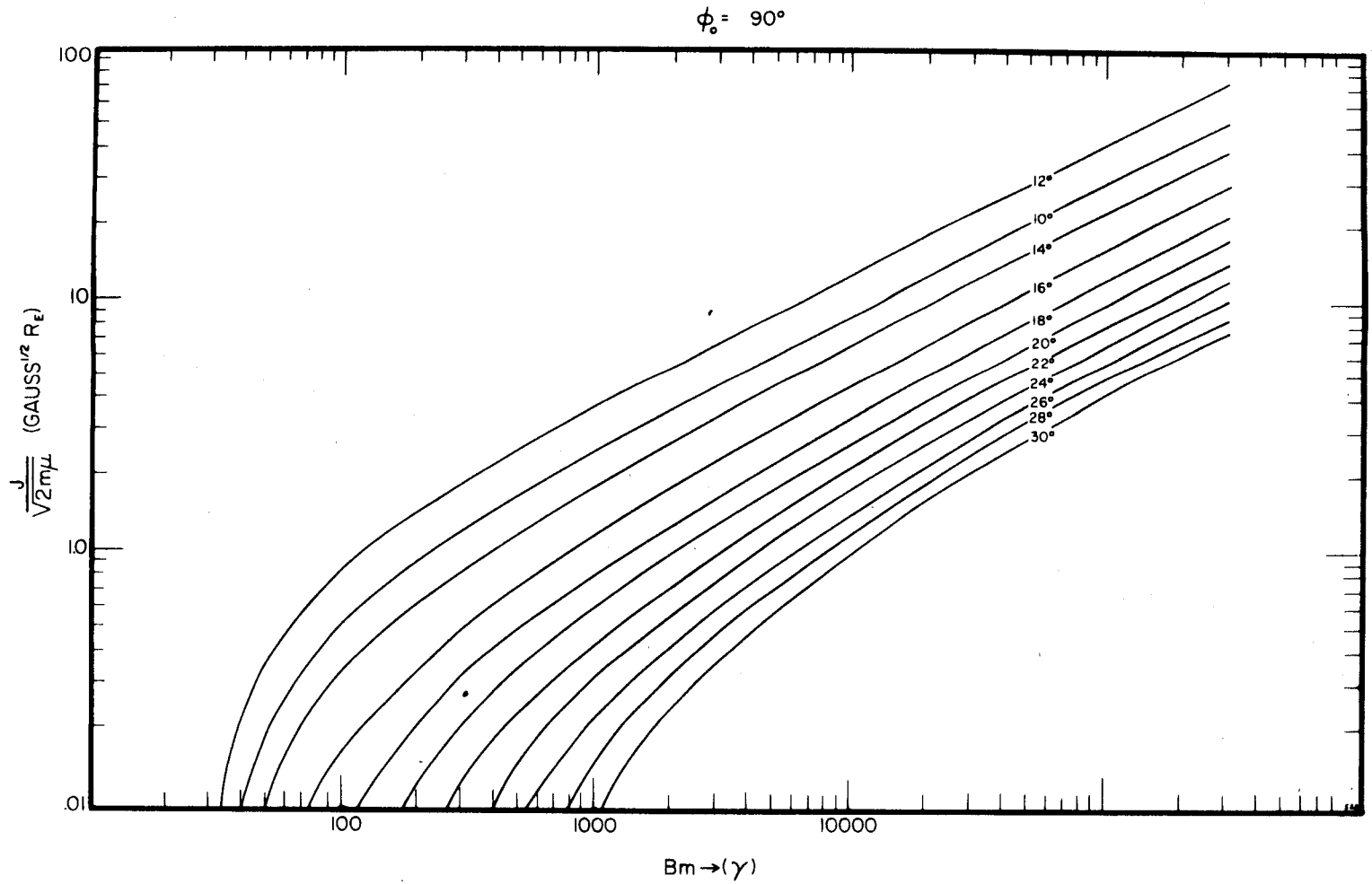
ϕ_o = 90°
100
10
1.0
.01
$\frac{J}{\sqrt{2m\mu}}$ (GAUSS$^{1/2}$ R_E)
12°
10°
14°
16°
18°
20°
22°
24°
26°
28°
30°
100
1000
10000
Bm → (γ)

FIGURE 10

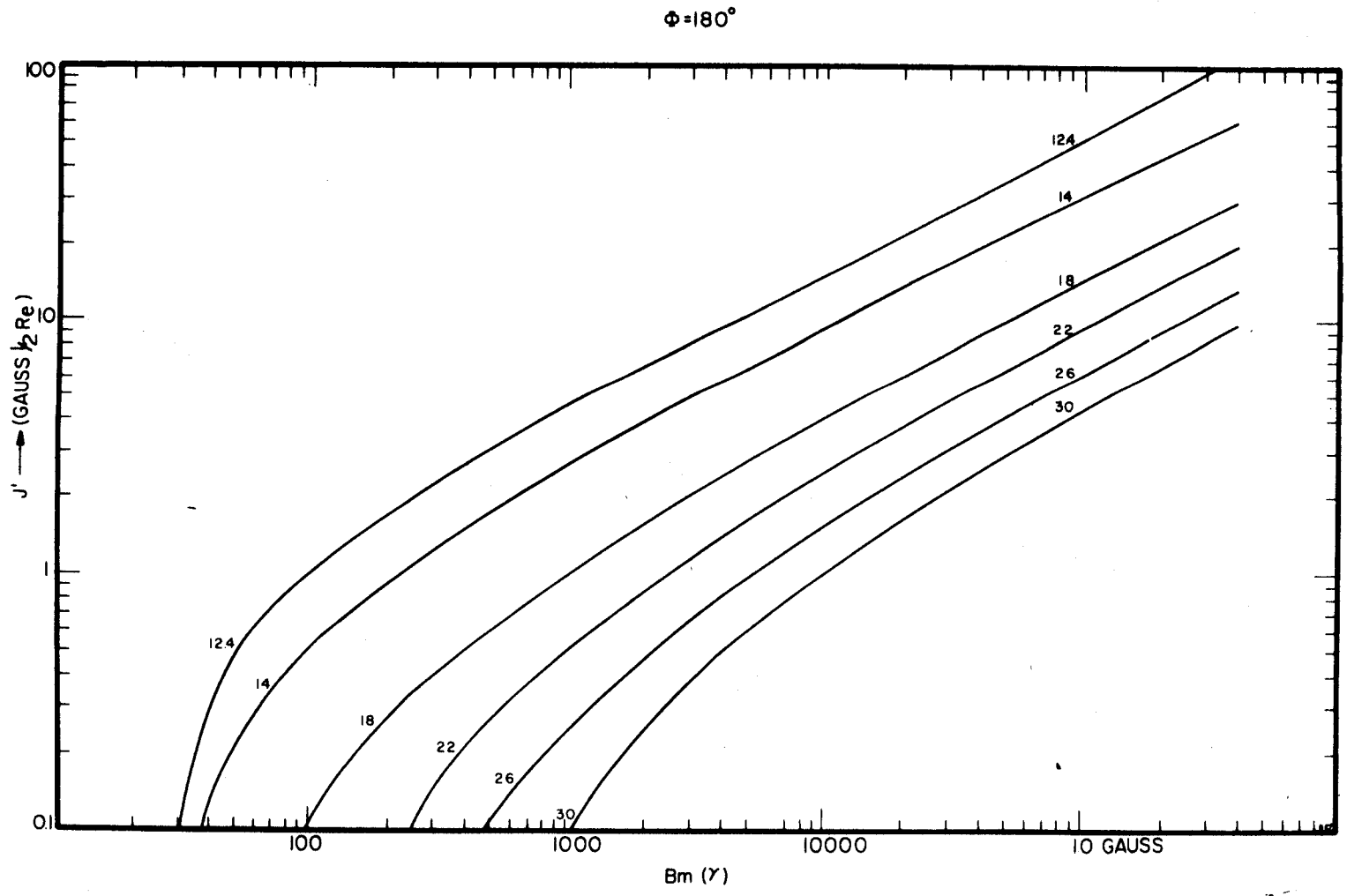
Φ=180°
100
10
1
0.1
J' ⟶ (GAUSS ½ Re)
124
14
18
22
26
30
100
1000
10000
10 GAUSS
Bm (Y)

Figure 11

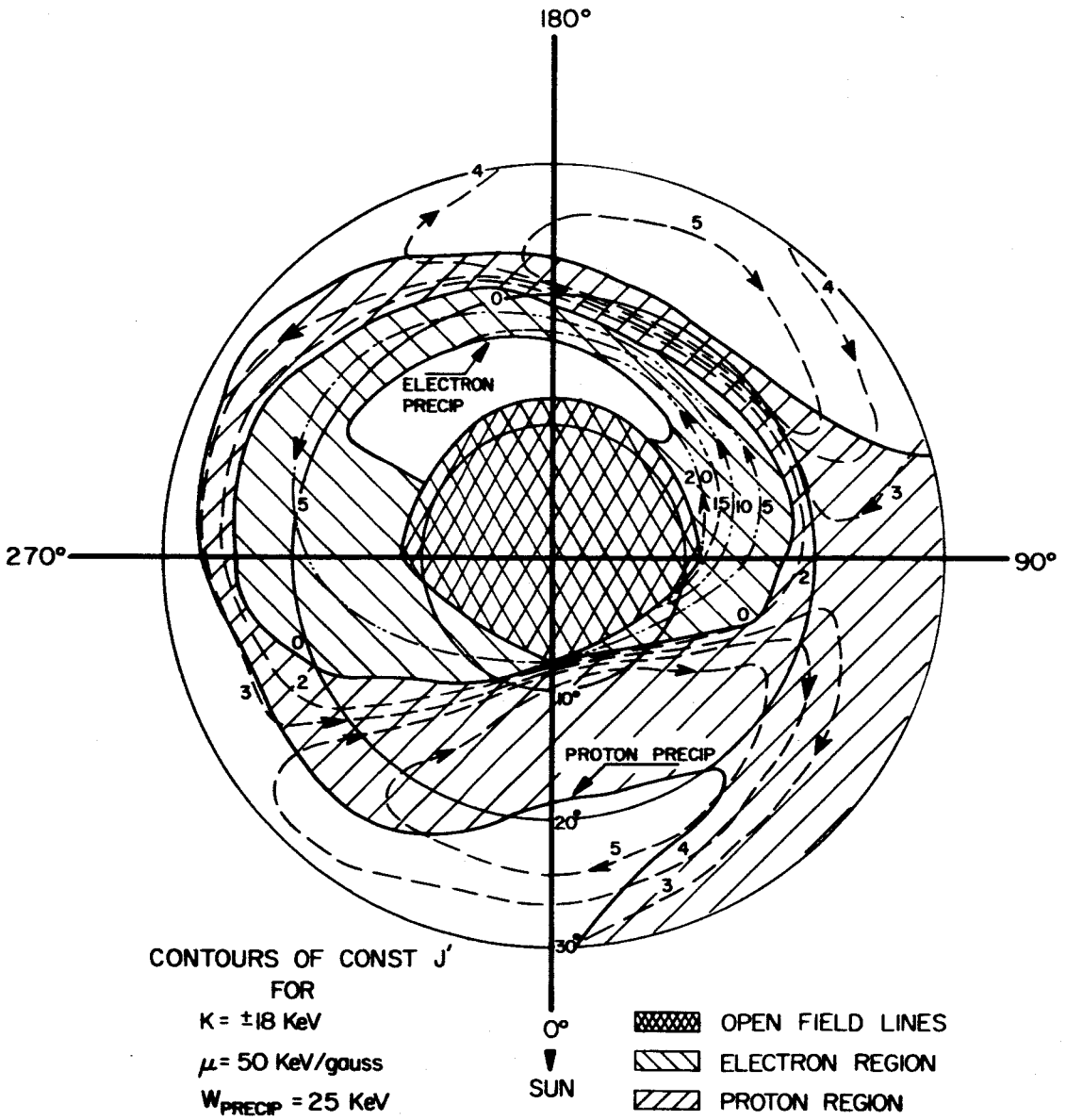
180°
270°
90°
0°
SUN
ELECTRON PRECIP
PROTON PRECIP
CONTOURS OF CONST J'
FOR
K = ±18 KeV
μ = 50 KeV/gauss
W PRECIP = 25 KeV
OPEN FIELD LINES
ELECTRON REGION
PROTON REGION

Figure 12

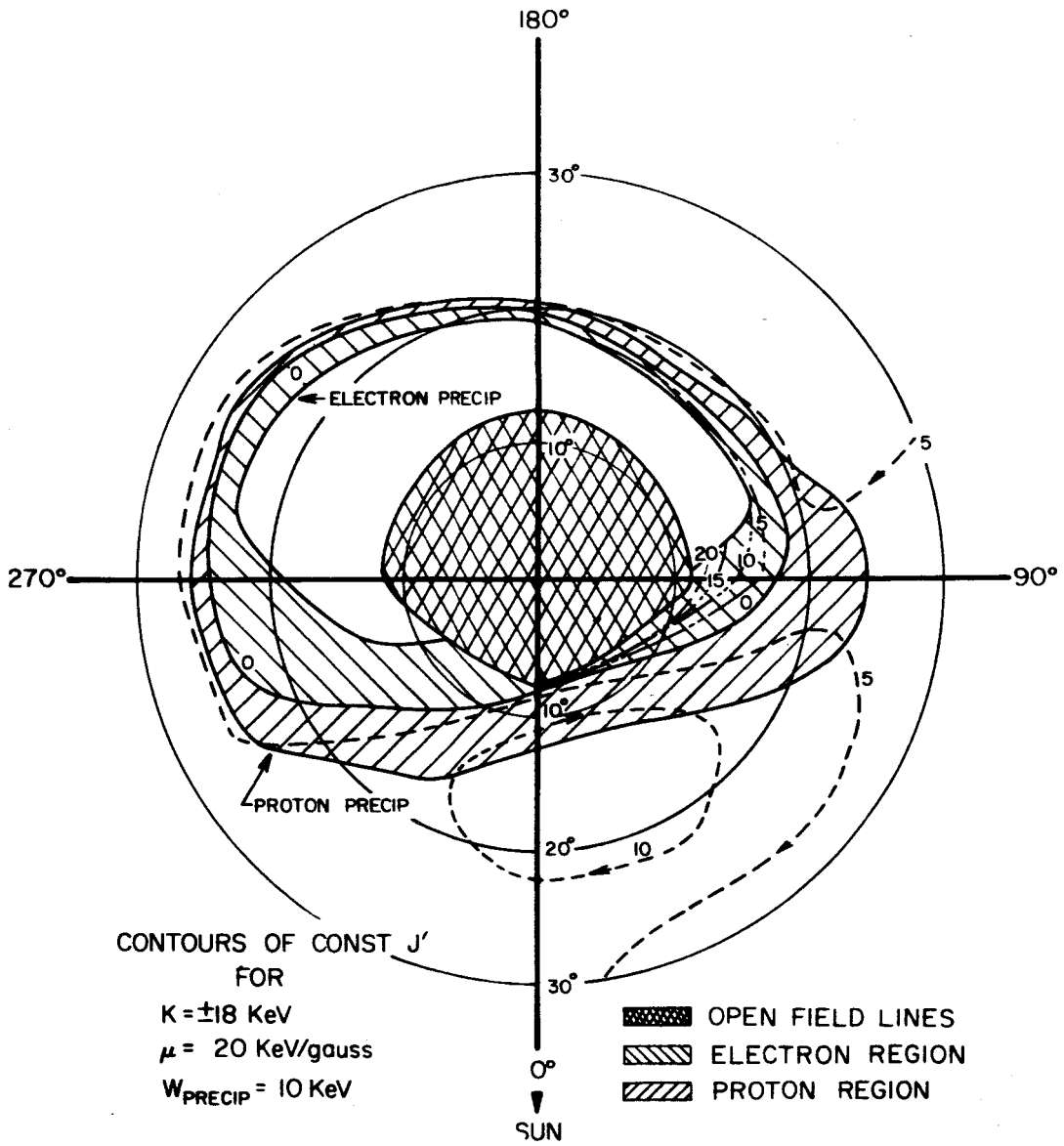
180°
30°
270°
90°
0°
SUN
ELECTRON PRECIP
PROTON PRECIP
0
5
10
15
20
CONTOURS OF CONST J'
FOR
K = ±18 KeV
μ = 20 KeV/gauss
W_PRECIP = 10 KeV
OPEN FIELD LINES
ELECTRON REGION
PROTON REGION

Figure 13

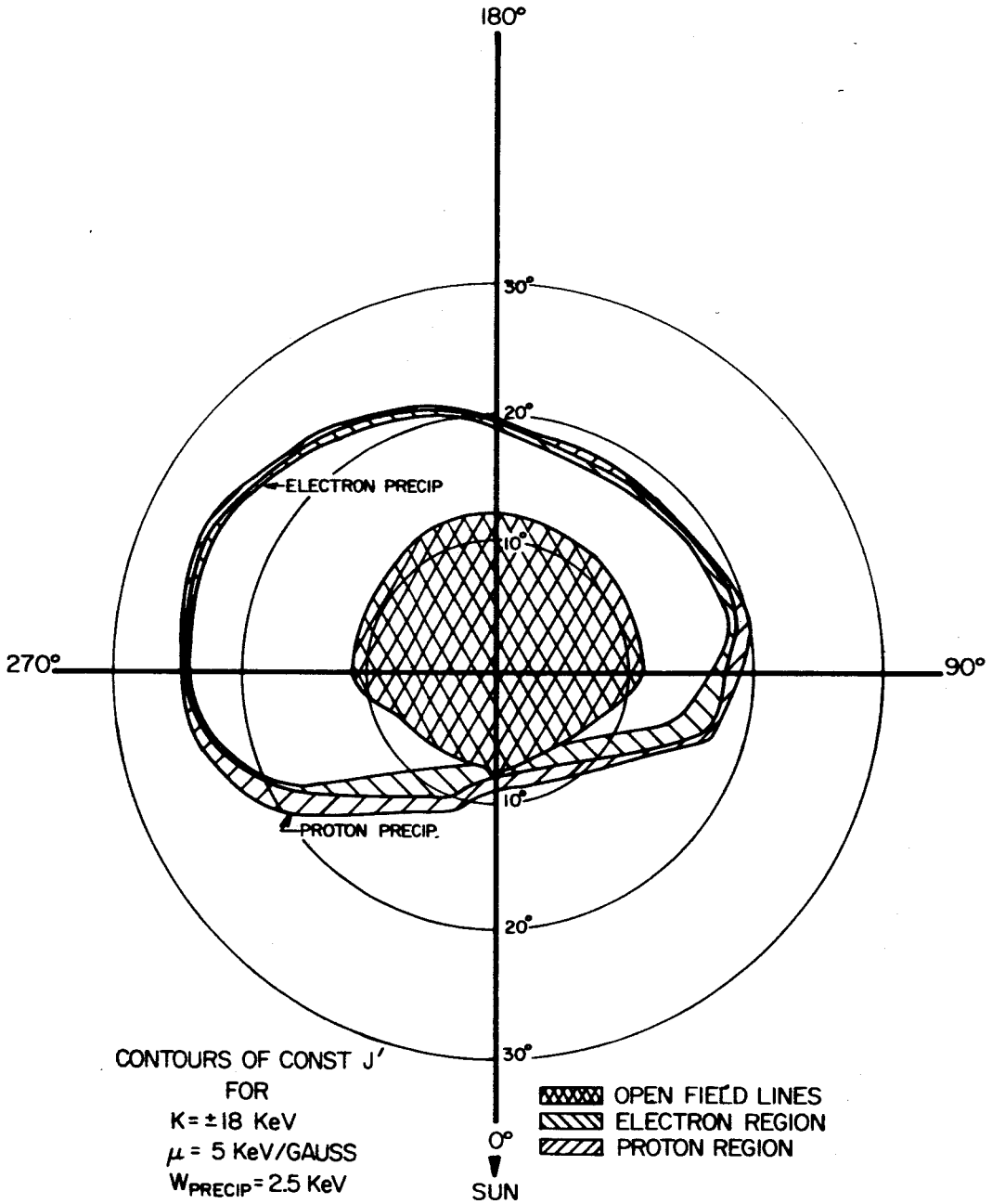
180°
30°
20°
ELECTRON PRECIP
10°
270°
90°
10°
PROTON PRECIP.
20°
30°
CONTOURS OF CONST J'
FOR
K = ± 18 KeV
μ = 5 KeV/GAUSS
W PRECIP = 2.5 KeV
0°
SUN
OPEN FIELD LINES
ELECTRON REGION
PROTON REGION

Figure 14

PRECIPITATION REGIONS FOR SOLAR WIND PARTICLES

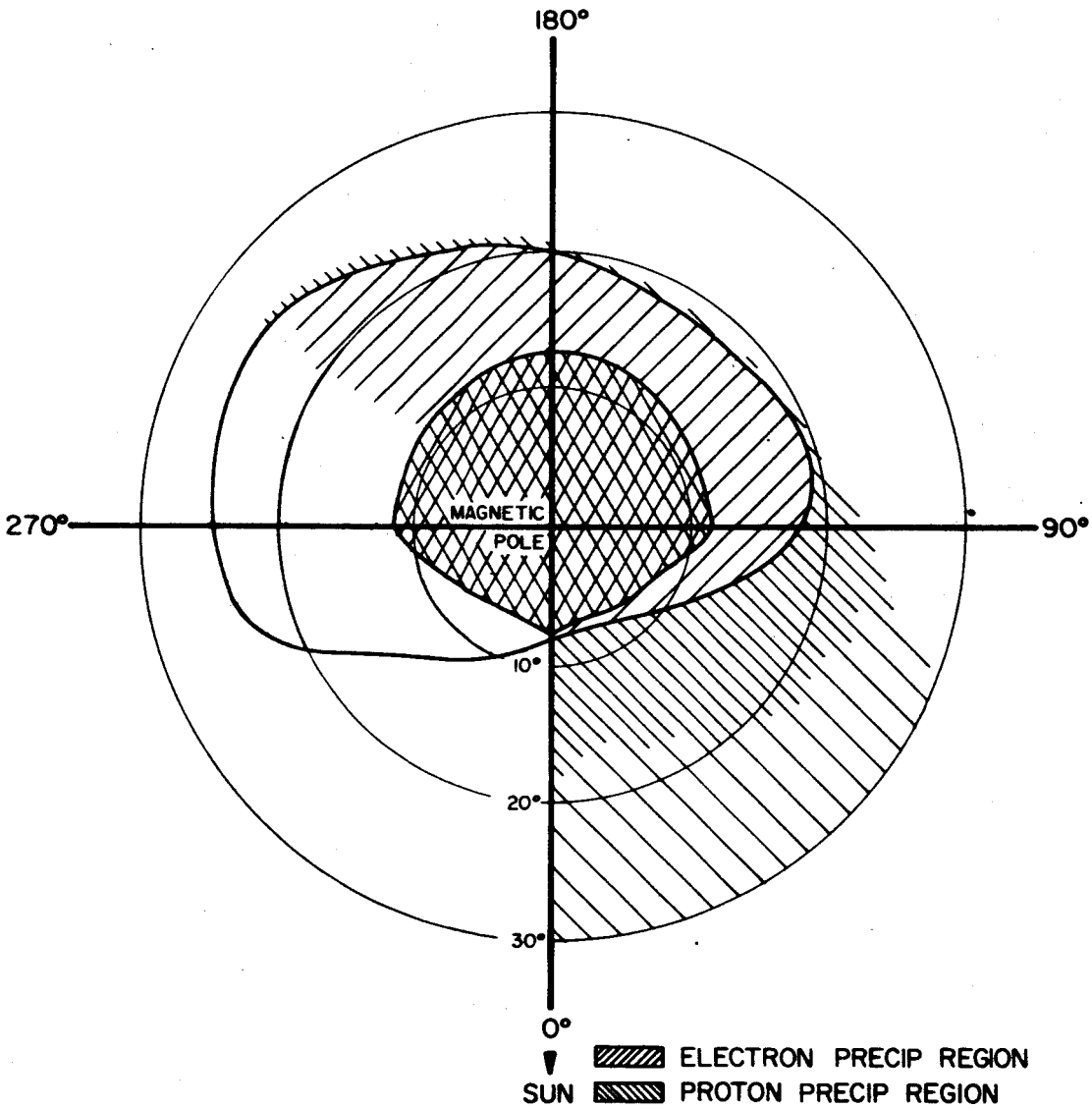

FIGURE 15

COMPARISON OF PRECIPITATION REGION WITH OBSERVED FLUXES OF

$j(E_e \gtrsim 10\ KeV) \gtrsim 2.5 \times 10^7 \frac{electrons}{(cm^2\ sec\ sterad)}$

ADAPTED FROM FRITZ & GURNETT

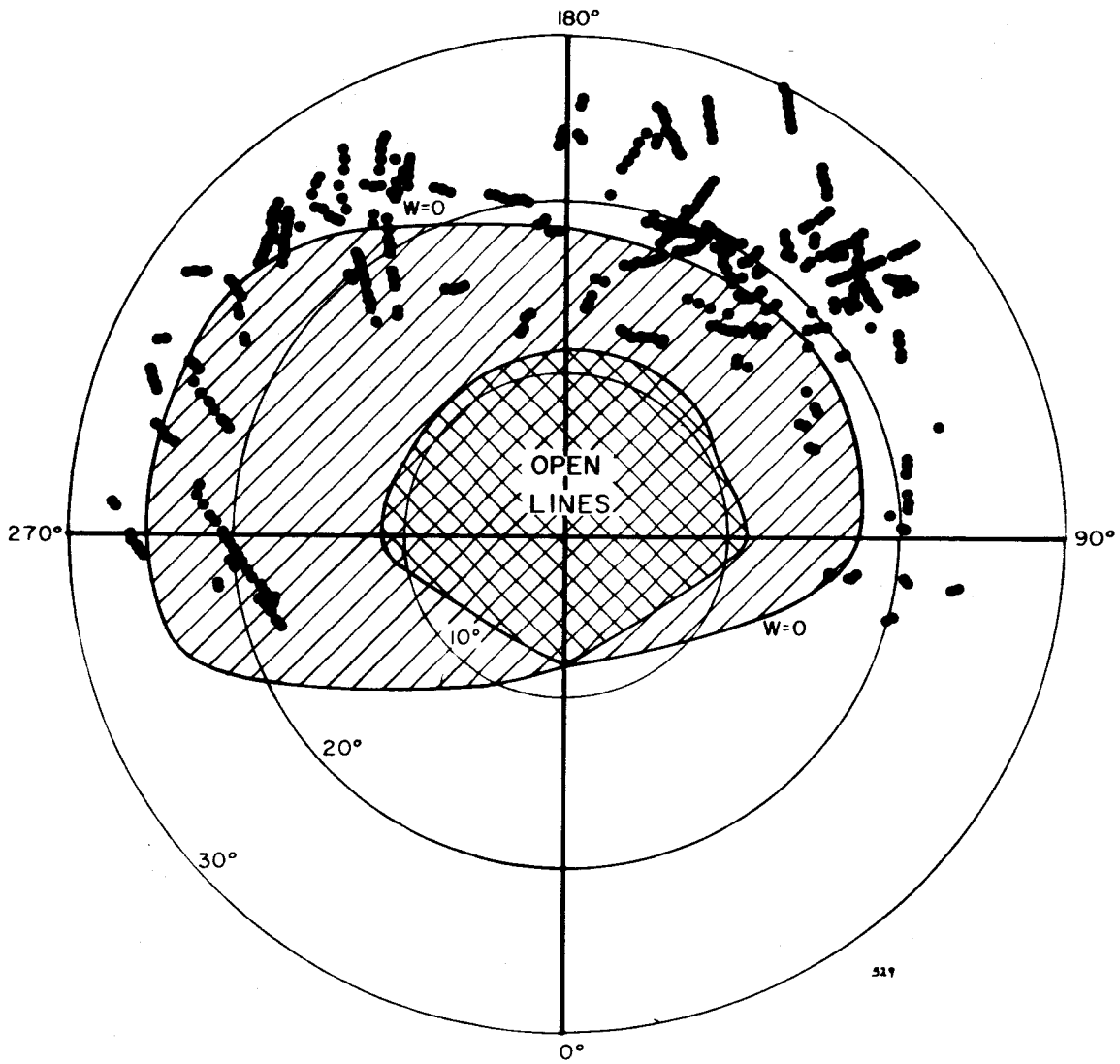

Figure 16